THE JOURNAL OF BIOLOGICAL CHEMISTRY VOL. 284, NO. 2, pp. 807–817, January 9, 2009

Riplet/RNF135, a RING Finger Protein, Ubiquitinates RIG-I to Promote Interferon-β Induction during the Early Phase of Viral Infection*[S]

Received for publication, June 3, 2008, and in revised form, November 10, 2008 Published, JBC Papers in Press, November 18, 2008, DOI 10.1074/jbc.M804259200

Hiroyuki Oshiumi[‡], Misako Matsumoto[‡], Shigetsugu Hatakeyama[§], and Tsukasa Seya[‡1]

From the [‡]Department of Microbiology and Immunology and the [§]Department of Biochemistry, Hokkaido University Graduate School of Medicine, Kita-15, Nishi-7, Kita-ku Sapporo 060-8638, Japan

RIG-I (retinoic acid-inducible gene-I), a cytoplasmic RNA helicase, interacts with IPS-1/MAVS/Cardif/VISA, a protein on the outer membrane of mitochondria, to signal the presence of virus-derived RNA and induce type I interferon production. Activation of RIG-I requires the ubiquitin ligase, TRIM25, which mediates lysine 63-linked polyubiquitination of the RIG-I N-terminal CARD-like region. However, how this modification proceeds for activation of IPS-1 by RIG-I remains unclear. Here we identify an alternative factor, Riplet/RNF135, that promotes RIG-I activation independent of TRIM25. The Riplet/RNF135 protein consists of an N-terminal RING finger domain, C-terminal SPRY and PRY motifs, and shows sequence similarity to TRIM25. Immunoprecipitation analyses demonstrated that the C-terminal helicase and repressor domains of RIG-I interact with the Riplet/RNF135 C-terminal region, whereas the CARD-like region of RIG-I is dispensable for this interaction. Riplet/RNF135 promotes lysine 63-linked polyubiquitination of the C-terminal region of RIG-I, modification of which differs from the N-terminal ubiquitination by TRIM25. Overexpression and knockdown analyses revealed that Riplet/RNF135 promotes RIG-I-mediated interferon-β promoter activation and inhibits propagation of the negative-strand RNA virus, vesicular stomatitis virus. Our data suggest that Riplet/RNF135 is a novel factor of the RIG-I pathway that is involved in the evoking of human innate immunity against RNA virus infection, and activates RIG-I through ubiquitination of its C-terminal region. We infer that a variety of RIG-I-ubiquitinating molecular complexes sustain RIG-I activation to modulate RNA virus replication in the cytoplasm.

Cytoplasmic viral RNA sensors induce production of type I interferon (IFN)[2] (1, 2). Representative cytoplasmic sensors, RIG-I-like receptors (RLRs) of RIG-I, MDA5, and LGP2, belong to the DEA(D/H) box RNA helicase family (3–6). RIG-I recognizes the 5′ end triphosphate of the virus RNA genome or double-stranded RNA (6–8) to sense infection by various RNA viruses (3, 5). The RIG-I protein consists of two N-terminal CARD-like domains, an RNA helicase region and a repressor domain (RD) (9). After recognition of positive or negative single-stranded viral RNA, RIG-I interacts with its adaptor molecule IPS-1/MAVS/Cardif/VISA leading to type I IFN production, thereby protecting host cells from amplified viral replication (10–13). However, only a few copies of viral RNAs usually penetrate the cell membrane to enter the cell at an early infection, and these RLRs are barely present in intact as well as early virus-infected cells (6). The early viral RNA recognition facility should be different from that of the late phase when RIG-I protein is abundant in the cytoplasm and easily re-organizes the virus RNAs. What molecular mechanism is responsible for initial sensing of viral RNA thus remains unknown.

Other RLRs, MDA5 and LGP2, are structurally similar to RIG-I in their having the helicase domain (5, 14). However, MDA5 lacks the RD domain although it possesses CARD-like region at the N terminus like RIG-I. LGP2 does not have a CARD-like region but possesses RD at its C terminus (9). RIG-I and MDA5 recognize different kinds of RNA viruses and in some cases play a redundant role in sensing virus infection, such as influenza B (15). In contrast, LGP2 rather negatively regulates virus replication. LGP2 expression suppressed RIG-I or MDA5 signaling (14, 16), and *lgp2* gene disruption conferred high susceptibility to virus infection on mice (4).

Recently, the majority of proteins involved in the type I IFN-inducing system were found ubiquitinated. For example, the tumor necrosis factor receptor-associated family members, TRAF3 and TRAF6, are ubiquitin ligases to induce ubiquitination of proteins and implicated in activation of IFN regulatory factor (IRF) 3 or nuclear factor (NF) κB (13, 17–19). In contrast, a deubiquitinating enzyme, DUBA or A20, suppresses these signals (19, 20). In addition to ubiquitin, ubiquitin-like protein, ISG15, is also conjugated to proteins involved in the IFN-inducing pathway (21, 22). Recent studies have revealed that viral RNA sensors are also ubiquitinated. TRIM25 (ZNF147 or EFP), a member of the ubiquitin-protein isopeptide ligase family, which possesses a RING finger domain, ubiquitinates the

* This work was supported in part by grants-in-aid from the Ministry of Education, Science and Culture of Japan, Ministry of Health, Labour, and Welfare, The Mitsubishi Foundation, and The Mochida Memorial Foundation. The costs of publication of this article were defrayed in part by the payment of page charges. This article must therefore be hereby marked "*advertisement*" in accordance with 18 U.S.C. Section 1734 solely to indicate this fact.

[S] The on-line version of this article (available at http://www.jbc.org) contains supplemental Figs. S1–S6.

The nucleotide sequence(s) reported in this paper has been submitted to the GenBank™/EBI Data Bank with accession number(s) AB470605.

[1] To whom correspondence should be addressed: Dept. of Microbiology and Immunology, Graduate School of Medicine, Hokkaido University, Kita-ku, Sapporo 060-8638, Japan. Tel.: 81-11-706-5073; Fax: 81-11-706-7866; E-mail: seya-tu@pop.med.hokudai.ac.jp.

[2] The abbreviations used are: IFN, interferon; RT, reverse transcription; RLR, RIG-I-like receptor; HA, hemagglutinin; siRNA, small interference; m.o.i., multiplicity of infection; VSV, vesicular stomatitis virus; IRF, IFN regulatory factor; Ub, ubiquitin; ORF, open reading frame; RD, repressor domain.

CARD-like domains of RIG-I thereby facilitating the RIG-I-mediated activation of type I IFN signaling (23, 24), although Shimotohno and co-workers (25) previously reported that TRIM25 (EFP) does not polyubiquitinate the RIG-I CARD-like region as far under their conditions. Expression of TRIM25 increases RIG-I CARD-like region-mediated signaling; however, it remains to be determined whether the activation of full-length RIG-I requires other ubiquitin ligase (23). Another ubiquitin ligase RNF125 mediates lysine 48-linked polyubiquitination of RIG-I, which leads to degradation of RIG-I through the proteasome (25).

Here we examined what molecular complex participates in an early RIG-I-mediated RNA recognition and IFN signaling by yeast two-hybrid screening. Here we detected two novel RING finger proteins that bound to RIG-I, and we found that one, RNF135, facilitated RIG-I-mediated type I IFN induction via ubiquitinating RIG-I. RNF135 plays a crucial role in the RIG-I response to minimal copies of viral RNA, and by binding to the C-terminal helicase and RD regions of RIG-I, RNF135 facilitates RIG-I C-terminal ubiquitination to up-regulate RIG-I-mediated IFN signaling and suppress viral replication. Hence, we renamed it as RNF135 Riplet (RING finger protein leading to RIG-I activation). To our knowledge, this is the first study demonstrating that C-terminal ubiquitination of RIG-I is important for full IFN induction by RIG-I.

EXPERIMENTAL PROCEDURES

Cell Cultures—HEK293 and Vero cells were cultured in Dulbecco's modified Eagle's medium with 10% fetal calf serum (Invitrogen), and HeLa cells were in minimum Eagle's medium with 2 mM L-glutamine and 10% fetal calf serum (JRH Biosciences). HEK293FT cells were maintained in Dulbecco's modified Eagle's high glucose medium containing 10% heat-inactivated fetal calf serum (Invitrogen).

Plasmids—cDNA fragment encoding a C-terminal region of Riplet was isolated by yeast two-hybrid screening using human lung cDNA library. The 5′ region encoding the remaining N-terminal region was amplified by PCR using primers Riplet-F1 and Riplet-R1, and human lung cDNA library was used for its template. Two cDNA fragments, which cover the entire ORF of Riplet, were joined by PCR using primers Riplet-F1, R1, F2, and R2 and then inserted into pCR-blunt vector (Invitrogen). The primers sequences are as follows: F1, GCCTCGAGGCCACCATGGCGGGCCTGGGCCTGGG; R1, CGGCCAGGTCCTGCAGTAGC; F2, GCACCTGCGGAAGAACACGC; and R2, GGGGATCCCACCTTTACTTGCTTTATTATCAGG. The obtained cDNA was cloned into XhoI-NotI restriction sites of pEF-BOS expression vector, and the HA tag was fused at the C-terminal end of Riplet. Riplet-DN (dominant negative) expression vector was constructed by amplifying the relevant Riplet cDNA fragment using the primers Riplet-X-F-C and Riplet-R2 and subcloned into pEF-BOS. The primer sequence of Riplet-X-F-C was as follows: GCTCGAGGCCACCATGCCGCACCTGCGGAAGAACACGC. Riplet-L248fs expression vector was made by deleting 1 base at position 742 by standard PCR-mediated site-directed mutagenesis methods with primers Riplet-L248fs-F and Riplet-L248fs-R as follows: Riplet-L248fs-F, CCAGAGCCACCCTGCATCAGGAGAGCTTCTCGG, and Riplet-L248fs-R, CCGAGAAGCTCTCCTGATGCAGGGTGGCTCTGG. All cloned *RIPLET* cDNA fragments were sequenced, and it was confirmed that there were no mutations. Full-length RIG-I expressing vector, Gal4-IRF-3, Gal4-DBD, and p55 UASG-Luc reporter plasmids were gifts from Dr. T. Fujita (Kyoto University, Kyoto, Japan). p125 luc reporter plasmid was a gift from Dr. T. Taniguchi (University of Tokyo, Tokyo, Japan). RIG-I RD expressing vector was made with primers RIG-I RD-F and RIG-I RD-R; the RIG-I dRD cDNA fragment, which encodes ORF of RIG-I from the 1- to 754-amino acid region, was made by using primers RIG-I-(1–754)F and RIG-I-(1–754)R. The obtained cDNA fragments were sequenced, and it was confirmed that there were no mutations caused by PCR. The primers sequences are as follows: RIG-I RD-F, GAT GAT AAA GGT ACC ACC GGT AGC AAG TGC TTC CTT CTG; RIG-I RD-R, AAG GAA GCA CTT GCT ACC GGT GGT ACC TTT ATC ATC ATC ATC; RIG-I-(1–754)F, GC AGA GGA AGA GCA AGA TGA TAT CAG GTC CTC AAT CTT C; and RIG-I-(1–754)R, ATT GAG GAC CTG ATA TCA TCT TGC TCT TCC TCT GCC TC.

Northern Blotting—Human *RIPLET* 1092-bp cDNA fragment (208–1299) was used for the probe for Northern blotting. The Northern blot membranes, human 12-lane MTN blot and MTN blot III, were purchased from Clontech. The homology of human *RIPLET* and *TRIM25* in the probe region was 46%. We used a stringent condition for Northern blotting to exclude the cross-hybridization between the *RIPLET* and *TRIM25* genes. Briefly, the probe was labeled with [α-^{32}P]dCTP using Rediprime II Random Prime labeling system (GE Healthcare). The labeled probe was hybridized to the membrane with ExpressHyb hybridization solution (Clontech) at 68 °C for 1 h. The membrane was washed with washing solution I (2× SSC, 0.05% SDS) for 40 min, and then washed with washing solution II (0.1× SSC, 0.1% SDS) for 40 min. Riplet mRNA bands were detected with x-ray film.

Reporter Gene Analysis—HEK293 cells were transiently transfected in 24-well plates using FuGENE HD (Roche Applied Science) with expression vectors, reporter plasmids, and internal control plasmid coding *Renilla* luciferase. The total amounts of plasmids were normalized with empty vector. For poly(I-C) stimulation, 24 h after transfection, cells were stimulated with medium containing poly(I-C) (50 μg/ml) and DEAE-dextran (0.5 mg/ml) for 1 h, and then the medium was exchanged with normal medium and incubated for an additional 3 h. Cells were lysed with lysis buffer (Promega) and luciferase, and *Renilla* luciferase activities were measured by the dual luciferase assay kit (Promega). Relative luciferase activities were calculated by normalizing luciferase activity by *Renilla* luciferase activity, and dividing the normalized value by control in which only empty vector, reporter, and internal control plasmid were transfected. Values are expressed as mean relative stimulations ± S.D. for a representative experiment, and each was performed three times in duplicate (unless otherwise indicated in the legends).

RNA Interference—Reporter and siRNA (20 nM final concentration) for Riplet or control were transfected into HEK293 cells with Lipofectamine 2000 (Invitrogen) by the standard method described in the manufacturer's protocol. Empty vec-

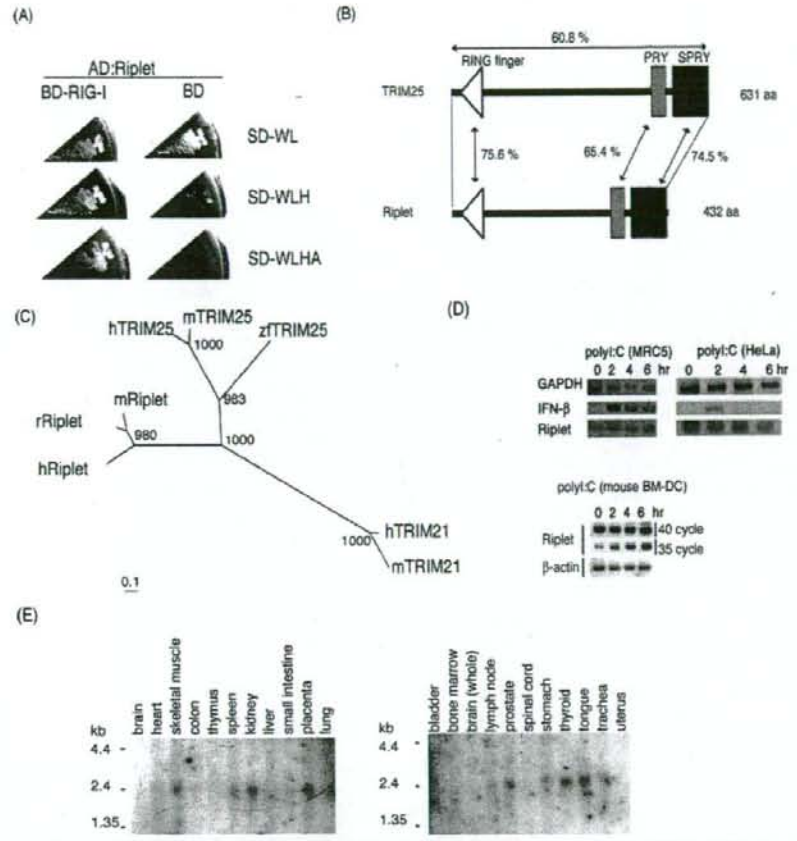

FIGURE 1. **Isolation of Riplet by yeast two-hybrid screening.** *A*, yeast cells carrying both RIG-I and Riplet can grow in selective media (SD-WLH, SD-WLHA), whereas yeast cells carrying RIG-I alone only grow in nonselective media (SD-WL), indicating the physical interaction of RIG-I with Riplet. *B*, human Riplet protein sequence is 60.8% identical to human TRIM25. The RING finger domains and SPRY motifs show higher sequence similarities between the two proteins. *aa*, amino acids. *C*, phylogenetic tree constructed by the Neighbor-Joining method shows that Riplet is similar to TRIM25. *h*, *m*, *r*, or *zf* represent human, mouse, rat, or zebrafish, respectively. The *numbers* on the node are bootstrap probabilities (n = 1000). *D*, HeLa cell, human primary-cultured fibroblast cell, MRC5, or bone marrow-derived mouse dendritic cell (*BM-DC*) were stimulated with poly(I-C) (50 μg/ml) for indicated hours. Total RNA was extracted with TRIzol reagent, and then RT-PCR was carried out using primers shown under "Experimental Procedures." *GAPDH*, glyceraldehyde-3-phosphate dehydrogenase. *E*, Northern blot membranes containing 1 μg of poly(A)$^+$ RNA per lane from human tissues were blotted with human Riplet probe.

tor was added to normalize the final plasmid amount. 48 h after transfection, cells were stimulated with poly(I-C) for 4 h. For VSV infection, 24 h after transfection, cells were infected with VSV at m.o.i. = 1, and cell lysate was prepared after 12 h for reporter gene assays. The degree of gene silencing was confirmed by RT-PCR using RNA extracted from cells 24 h after transfection. PCR primers used for the RT-PCR were Riplet-F3 (ACTGGGAAGTGGACACTAGG) and Riplet-R3 (ACTCATACAGAAGCTTCTCC). siRNAs were purchased from Funakoshi Co., Ltd. (Tokyo Japan), and the siRNA sequences of Riplet siRNA were GACUAUGGACUCUUGUUGUGU (sense) and ACAACAAGAGUCCAUAGUCCU (antisense). Control siRNA sequences were CUGUUGGUUUAGUAAGCCUGU (sense) and AGGCUUACUAAACCAACAGUC (antisense). Another siRNA, Riplet si-1, and control negative siRNA (silencer negative control 1 siRNA, AM4611) were purchased from Applied Biosystems. siRNA sequences were Riplet si-1 GGGAAAGCUUGCCUUCUAUdTdT (sense) and AUAGAAGGCAAGCUUUCCCdTdC (antisense).

Virus Preparation and Infection—VSV Indiana strain and poliovirus were amplified using Vero cells. HEK293 cells were transfected in 24-well plates with plasmid encoding *RIG-I*, Riplet, or no insert. 24 h after transfection, cells were infected with viruses for 24 h, and the titers of virus in culture supernatant were measured by plaque assay using Vero cells. For RNA interference assay, cells were transfected with siRNA with Lipofectamine 2000. 24 h after transfection, cells were infected with viruses at m.o.i. = 0.001 for 18 h, and the titer in culture supernatant were determined by plaque assay.

Immunoprecipitation—HEK293FT cells were transfected in 6-well plates with plasmids encoding FLAG-tagged RIG-I and/or HA-tagged Riplet. The plasmid amounts were normalized by the addition of empty plasmid. 24 h after transfection, cells were lysed with lysis buffer (20 mM Tris-HCl (pH 7.5), 125 mM NaCl, 1 mM EDTA, 10% glycerol, 1% Nonidet P-40, 30 mM NaF, 5 mM Na_3VO_4, 20 mM iodoacetamide, and 2 mM phenylmethylsulfonyl fluoride), and then proteins were immunoprecipitated with rabbit anti-HA polyclonal (Sigma) or anti-FLAG M2 monoclonal antibody (Sigma). The precipitated samples were analyzed by SDS-PAGE and stained with anti-HA (HA1.1) (Covance) or anti-FLAG M2 monoclonal antibody. For ubiquitination assay of RIG-I, the plasmid encoding two multiple HA-tagged ubiquitins was used. HEK293FT cells were transfected with plasmids encoding FLAG-tagged RIG-I, Riplet, or 2× HA-tagged ubiquitin. 24 h after transfection, cells were lysed, and then RIG-I was immunoprecipitated as described above. The samples were analyzed by SDS-PAGE and stained with anti-HA polyclonal antibody (for detection of ubiquitination) or anti-FLAG monoclonal antibody (for detection of RIG-I). Reproducibility was confirmed with additional experiments (see supplemental figures).

Construction of RIG-I 3KA and 5KA Mutant Genes—The C-terminal three or five lysine residues were mutated into alanines (designated as 3KA and 5KA). RIG-I 3KA has K888A, K907A, and K909A, whereas RIG-I 5KA has K849A, K851A,

K888A, K907A, and K909A. The mutant *rig-I* genes were made by PCR-mediated site-directed mutagenesis. The primers used for the PCR were as follows: K907–909A-forward, GTT CAG ACA CTG TAC TCG GCG TGG GCG GAC TTT CAT TTT GAG AAG, and K907–909A-reverse, CTT CTC AAA ATG AAA GTC CGC CCA CGC CGA GTA CAG TGT CTG AAC; K888A-forward, GAC ATT TGA GAT TCC AGT TAT AGC AAT TGA AAG TTT TGT GGT GGA GG, and K888A-reverse, CCT CCA CCA CAA AAC TTT CAA TTG CTA TAA CTG GAA TCT CAA ATG TC; K849–851A-forward, GAG TAG ACC ACA TCC CGC CCA GCG CAG TTT TCA AGT TTT G, and K849–851A-reverse, CAA AAC TTG AAA ACT GCG CTG GCG CGG GAT GTG GTC TAC TC. PCR was carried with Pyrobest *Taq* polymerase, and the obtained clones were sequenced to exclude the clones harboring PCR error. To construct the plasmid-expressing mutant RIG-I protein, the wild-type *RIG-I* gene on pEF-BOS vector was replaced with the mutant *rig-I* gene.

Real Time PCR—Quantitative PCR analyses were carried out using iCycler iQ real time detection system with Platinum SYBR Green qPCR SuperMix-UDG reagent (Invitrogen). Primer sequences for qPCR were as follows: hGAPDH-qF, GAG TCA ACG GAT TTG GTC GT, and hGAPDH-qR, TTG ATT TTG GAG GGA TCT CG; hIFN-β-qF, TGG GAG GAT TCT GCA TTA CC, and hIFN-β-qR, CAG CAT CTG CTG GTT GAA GA; hMx1-qF, ACC ACA GAG GCT CTC AGC AT, and hMx1-qR, CTC AGC TGG TCC TGG ATC TC; and hIFIT-1-qF, GCA GCC AAG TTT TAC CGA AG, and hIFIT-1-qR, CAC CTC AAA TGT GGG CTT TT. Values were expressed as mean relative stimulations, and for a representative experiment from a minimum of three separate experiments, each was performed in triplicate.

RESULTS

RIG-I-binding Proteins—To isolate the proteins that bind to RIG-I, we performed yeast two-hybrid screening using a human lung cDNA library. Using the RIG-I central region (213–601 amino acids), we isolated a clone that encoded a partial ORF of a gene expressed in a dendritic cell line, DC12, whereas the C-terminal region of RIG-I (557–925 amino acids) resulted in the isolation of two cDNA clones, which encoded partial C-terminal regions of ZNF598 and RNF135 (Fig. 1*A* and data not shown). Preliminary expression studies showed that the RNF135 segment affected the RIG-I IFN-β inducing activity, whereas the other two proteins had no effect (data not shown). We confirmed the

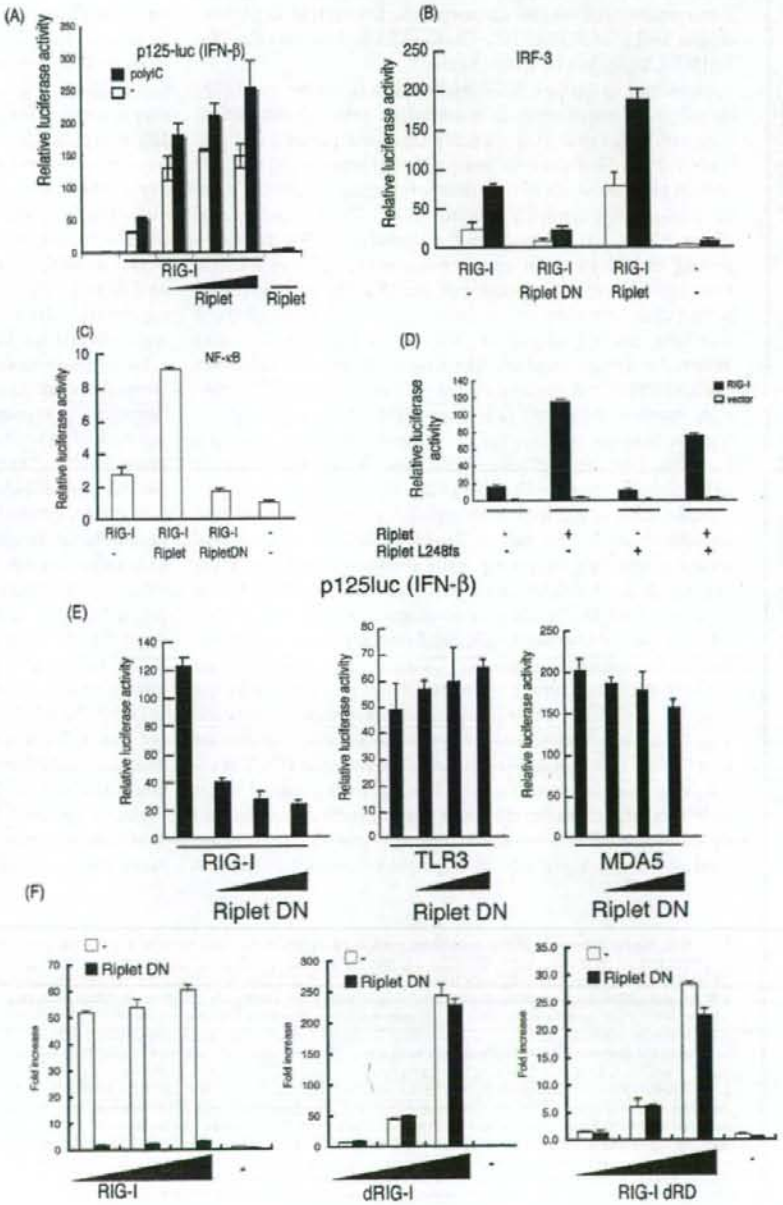

interaction of RIG-I with ZNF598 or RNF135 in HEK293FT cells by immunoprecipitation (data not shown). RNF135 was previously annotated by the genome project and was recently found to be a cause of a genetic disease, neurofibromatosis, although its protein function was unknown. We renamed the protein Riplet (RING finger protein leading to RIG-I activation) based on the following functional analyses. Riplet was most similar to TRIM25 (60.8% sequence homology), in particular between their RING finger domains PRY or SPRY (Fig. 1*B*). Phylogenetic analysis also supported the notion that Riplet was similar to TRIM25 (Fig. 1*C*). Thus, we hypothesized that, like TRIM25, Riplet is a ubiquitin ligase.

Expression of Riplet—RIG-I mRNA is induced by type I IFN or poly(I-C) stimulation in mammalian cells. Unlike RIG-I, however, Riplet mRNA was basally expressed in HeLa and primary-cultured MRC-5 cells irrespective of stimulation (Fig. 1*D* and data not shown). On the other hand, when we treated bone marrow-derived dendritic cells with poly(I-C), the basal level of Riplet mRNA was increased by the stimulation (Fig. 1*D*), suggesting that the regulatory mechanism of Riplet expression somewhat differs among cell types, and that Riplet is expressed before virus infection in some cell types. Next we performed Northern blotting of human tissue RNA. Riplet mRNA was detected as a single band of 2.4 kbp, which is slightly longer than the RNF135 cDNA sequence deposited in GenBank™ (accession number AB470605). Human *RIPLET* is expressed in human skeletal muscle, spleen, kidney, placenta, prostate, stomach, thyroid, and tongue and also weakly expressed in heart thymus, liver, and lung (Fig. 1*E*).

Riplet Enhances RIG-I-mediated IFN-β Induction—At first we characterized the role of Riplet in RIG-I-mediated IFN inducing signaling by reporter gene analyses. When RIG-I was expressed in HEK293 cells, reporter auto-activation was observed even in the absence of exogenous stimulation (Fig. 2*A*) as reported previously (25, 26). Stimulation with poly(I-C) further enhanced the promoter. Co-expression of Riplet with RIG-I potentiated activation of the IFN-β promoter, whereas expression of Riplet alone resulted in only marginal activation (Fig. 2*A*). Detection of endogenous IFN-β mRNA confirmed that Riplet enhanced RIG-I-mediated activation of IFN-β transcription (supplemental Fig. S1). The enhancing role of Riplet in IFN-β promoter activation was also supported by activation of IRF-3 and NF-κB by Riplet (Fig. 2, *B* and *C*). In contrast, expression of a Riplet partial fragment (Riplet-DN) (70–432 amino acids) that lacked the N-terminal RING finger domain reduced promoter activation (Fig. 2*E*). The Riplet-L249fs mutant protein, which was isolated from neurofibromatosis patients (27), did not increase the RIG-I-mediated promoter activation (Fig. 2*D*). These data indicate that Riplet augments RIG-I-mediated IFN-β promoter activation, and that both the RING finger domain and the C-terminal region encoding the SPRY and PRY motifs are important for its function. Riplet (residues 70–432) acted as a dominant-negative form (hereafter called Riplet-DN) (Fig. 2, *E* and *F, left panel*). This functional feature of Riplet-DN was confirmed in Fig. 2, *B* and *C*, and was later confirmed through RIG-I co-precipitation and ubiquitination analyses (see Fig. 5*C* and supplemental Fig. S4*C*). Expression of Riplet-DN did not reduce TLR3 or MDA5 signaling (Fig. 2*E*), suggesting that Riplet-DN is specific for RIG-I signaling. Interestingly, the Riplet-DN only partially suppressed the function of the C-terminal deleted RIG-I (dRD), which is a constitutively active form (Fig. 2*F, right panel*), and RIG-I CARD-like region (dRIG-I)-mediated signaling in high or low dose transfection of dRIG-I was barely inhibited by overexpression of Riplet-DN (Fig. 2*F, center panel*). These data suggest that Riplet requires the RIG-I C-terminal domain (RD) and partial helicase region to activate RIG-I signaling.

Endogenous Riplet Promotes the RIG-I Signaling—We performed Riplet knockdown by siRNA Riplet using Lipofectamine 2000 reagents, instead of FuGENE HD, to reveal the function of endogenous Riplet. Two siRNAs (Riplet siRNA and Riplet si-1) that target different sites of the Riplet mRNA and two control siRNAs were used for knockdown analyses. The two siRNA or control siRNA were co-transfected with HA-tagged Riplet expression vector into HEK293 cells, and after 48 h, cell lysate was prepared and analyzed by Western blotting with anti-HA antibody detecting Riplet. The two siRNAs targeting Riplet abolished exogenously expressed Ripelt-HA, but control siRNA did not (supplemental Fig. S3). Likewise, both Riplet siRNA and Riplet si-1 specifically down-regulate the level of endogenous Riplet mRNA (Fig. 3, *A* and *B*).

Using the siRNA, we examined whether Riplet knockdown reduces RIG-I signaling. As expected, RIG-I-mediated IFN-β promoter activation was reduced by Riplet siRNA or Riplet si-1 compared with control siRNA (Fig. 3, *A* and *B*), indicating that Riplet is required for full activation of the RIG-I signaling. Vesicular stomatitis virus (VSV) is a negative-stranded RNA virus that induces IFN-β production via RIG-I (3). Although the

FIGURE 2. **Riplet enhances IFN-β signaling mediated by RIG-I.** *A*, Riplet enhances the promoter activation by RIG-I. HEK293 cells were transfected with plasmids encoding empty vector, RIG-I (0.1 μg) and Riplet (0.025, 0.05, or 0.1 μg) together with p125-luc (IFN-β promoter) reporter plasmid in 24-well plates. 24 h after transfection, the cells were treated with mock or poly(I-C) (50 μg/ml) for 4 h as described under "Experimental Procedures," and then luciferase activities of cell lysates were measured. *Closed* or *open boxes* represent poly(I-C) or mock stimulation, respectively. *B*, to examine the activation of IRF-3, RIG-I (0.1 μg), Riplet (0.1 μg), and/or Riplet-DN (0.1 μg),expressing vectors were transfected into HEK293 cells with reporter plasmids, GAL4 fused IRF-3 (0.05 μg), and the p55 UASG-luc reporter gene (0.05 μg), in which luciferase reporter gene is fused downstream of GAL4 protein-binding site, and therefore activated IRF-3 promotes the transcription of luciferase reporter gene. The cells were stimulated with poly(I-C) as described above (34). The total amount of transfected DNA (0.5 μg/well) was kept constant by adding empty vector (pEF-BOS). *C*, HEK293 cells were transfected with RIG-I (0.1 μg), Riplet (0.1 μg), and/or Riplet-DN (0.1 μg) expressing vectors together with the NF-κB reporter plasmid (0.1 μg), and 24 h later, the luciferase activities of cell lysates were measured. *D*, Riplet-L248fs, which lacks the C-terminal region, did not enhance the activation at all. HEK293 cells were transfected with the plasmids expressing wild-type Riplet (0.1 μg) or Riplet-L248fs (0.1 μg) together with RIG-I expressing vector (0.1 μg) and p125-luc reporter (0.1 μg). 24 h after transfection, cell were stimulated with poly(I-C), and the luciferase activities of cell lysates were determined as described above. *E*, RIG-I (0.1 μg), MDA5 (0.1 μg), or TLR3 (0.1 μg) expressing vectors were transfected into HEK293 cells with the plasmid encoding the Riplet-DN fragment (0.1, 0.2, or 0.3 μg) in 24-well plates. After 24 h, the cells were stimulated with 50 μg of poly(I-C) for 4 h, and relative luciferase activities were determined. *F*, Riplet-DN (100 ng) was co-transfected with full-length RIG-I (0, 50, 100, or 200 ng), RIG-I CARD-like region (dRIG-I) (0, 50, 100, or 200 ng), or C-terminal deleted RIG-I (RIG-I dRD) (0, 50, 100, or 200 ng) into HEK293 cells in 24-well plate, and reporter gene assays were carried out.

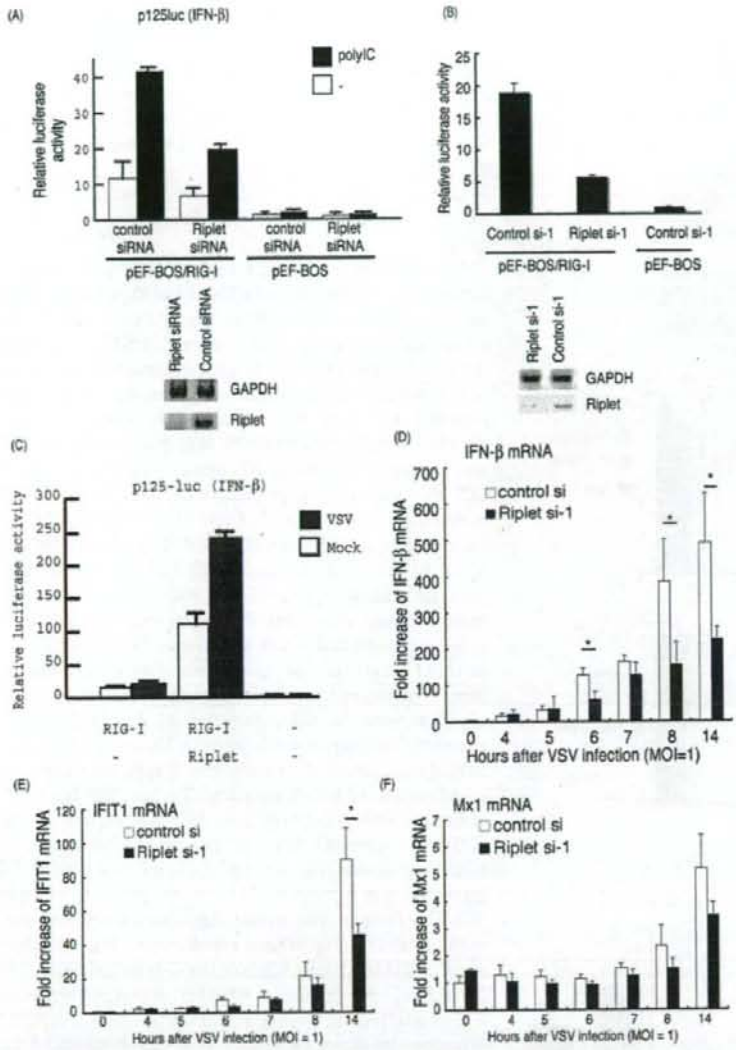

FIGURE 3. **Knockdown analyses of Riplet.** *A*, p125 luc reporter plasmid (0.1 μg), RIG-I expressing vector (0.1 μg), and Riplet siRNA or control siRNA (10 pmol), which were purchased from Funakoshi Co. Ltd., were transfected into HEK293 cells in a 24-well plate with Lipofectamine 2000, and 48 h after transfection, the cells were stimulated with poly(I-C) for 6 h, and the cell lysate was prepared, and luciferase activities were measured. RT-PCR was carried out using total RNA extracted from cells 48 h after transfection. *B*, p125 luc reporter plasmid (0.1 μg), RIG-I expressing vector (0.1 μg), and siRNA, Riplet si-1, or control si-1 (10 pmol), which were purchased from Applied Biosystems, were transfected into HEK293 cells with Lipofectamine 2000. 48 h after transfection, the cells were stimulated with poly(I-C) for 6 h. The cell lysate was prepared, and luciferase activities were measured. RT-PCR was carried out using total RNA extracted from cells 48 h after transfection. *C*, HEK293 cells were transfected with the plasmids expressing RIG-I (0.1 μg) and/or Riplet (0.1 μg) with p125 luc reporter plasmid (0.1 μg) in 24-well plates. After 24 h, the cells were infected with VSV (m.o.i. = 1) for 12 h. The luciferase activities of the cell lysates were measured. Expression of Riplet strongly enhanced IFN-β promoter activation by VSV through RIG-I. *D–F*, siRNA (control si- or Riplet si-1) were transfected into HEK293 cells, and after 48 h, the cells were infected with VSV at m.o.i. = 1. RNA was extracted at the indicated hours, and the quantitative PCR were carried out to detect the expression of IFN-β (*D*), IFIT-1 (*E*), or Mx1 (*F*) mRNA. *, $p < 0.05$. *GAPDH*, glyceraldehyde-3-phosphate dehydrogenase.

IFN-β promoter was only minimally activated by RIG-I in response to VSV (m.o.i. = 1) during the early phase of infection (<12 h), the activity was increased by RIG-I and Riplet (Fig. 3*C*). Riplet was silenced by siRNA and then VSV infected the cells. VSV-derived up-regulation of IFN-β mRNA was started around 6 h post-infection, and Riplet siRNA significantly suppressed the increase of IFN-β mRNA at 6 h (Fig. 3*D*). Because VSV infection is mainly sensed by RIG-I, this is consistent with the notion that Riplet promotes the RIG-I signaling. Other IFN-inducible genes, *IFIT1* and *MX1*, were expressed >8 h post-infection, and their expressions were also suppressed by Riplet siRNA (Fig. 3, *E* and *F*).

Riplet Exerts Protective Activity against Viral Infection—Next we examined the role of Riplet during viral infection. Riplet and/or RIG-I were transiently expressed in the human cells by FuGENE HD reagents, and then the cells were infected with VSV or poliovirus (a positive-stranded RNA virus). The viral titer of the supernatant was determined 24 h post-infection. Under our conditions, expression of RIG-I weakly inhibited VSV propagation. Co-expression of Riplet with RIG-I significantly suppressed VSV replication especially at low m.o.i., whereas Riplet alone did not suppress VSV (Fig. 4, *A* and *B*, *upper panel*). Therefore, a sufficient amount of RIG-I protein is required for Riplet to exert antivirus activity. This requirement of RIG-I is also observed in reporter gene analyses (Fig. 2). Under a similar setting, the antiviral effect of Riplet was marginally observed against poliovirus, which induces IFN-β largely via MDA5 (Fig. 4*B*, *lower panel*). To assess the importance of endogenous Riplet for antivirus effect of human cells, Riplet knockdown cells were infected with viruses. In Riplet knockdown cells, the VSV titer was consistently increased compared with the control ($p < 0.05$) (Fig. 4*C*, *left panel*). In addition, infection of Riplet knockdown cells with poliovirus resulted in only a slight increase in the poliovirus titer compared with the control ($p > 0.05$) (Fig. 4*C*, *right panel*). Because poliovirus is mainly recognized by MDA5 but not RIG-I, this marginal effect of Riplet on poliovirus infection was within expectation (3, 28).

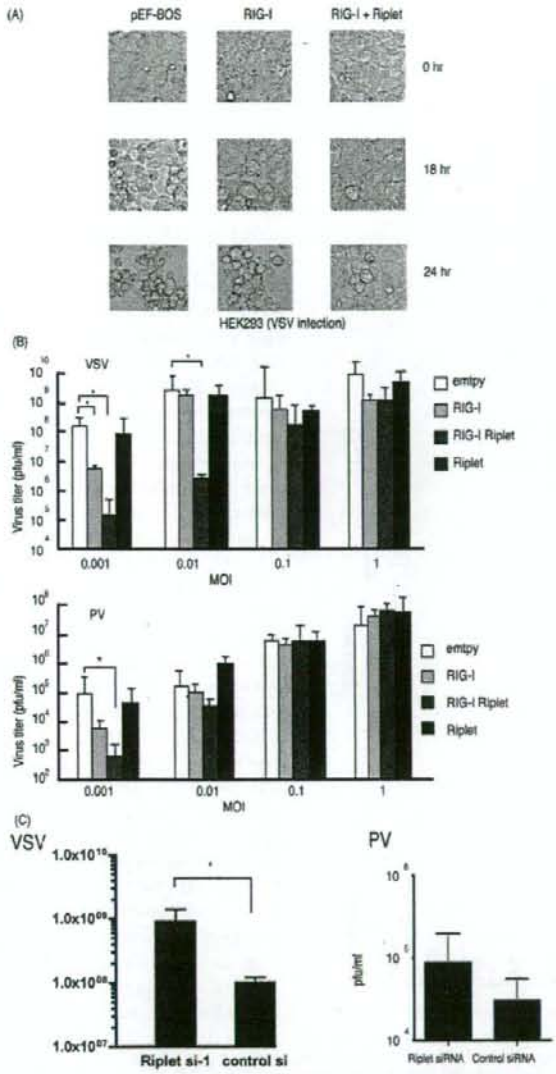

FIGURE 4. **Suppression of RNA viruses by Riplet.** *A*, HEK293 cells were transfected with RIG-I (0.1 μg) and/or Riplet (0.1 μg) expressing vectors. The total amount of transfected DNA (0.5 μg/well) in each well was kept constant by adding empty vector (pEF-BOS). 24 h after transfection, the cells were infected with VSV at m.o.i. = 0.1, and after 0, 18, or 24 h, CPE was observed by microscope. *B*, RIG-I (0.1 μg) and/or Riplet (0.1 μg) expressing plasmids were transfected to HEK293 cells in 24-well plates and incubated for 24 h. The total amount of transfected DNA (0.5 μg/well) in each well was kept constant by adding empty vector (pEF-BOS). The cells were infected with VSV (*upper panel*) or poliovirus (*PV*) (*lower panel*) at the indicated m.o.i. The viral titers in the culture media were measured 24 h after infection by plaque assay. *Error bars* represent standard deviation ($n = 3$). *, $p < 0.05$. *C*, control or Riplet knockdown HEK293 cells were infected with VSV (*left panel*) or poliovirus (*right panel*) at m.o.i. = 0.1. The viral titers in the culture media were measured 26 h after infection by plaque assays. Knockdown of Riplet induced higher VSV titers compared with control ($p < 0.05$), but the increase observed in poliovirus-infected Riplet knockdown cells was not significant ($p > 0.05$).

Riplet and Riplet-DN Bind the Helicase and RD Regions of RIG-I—Yeast two-hybrid analysis showed that a C-terminal region of Riplet bound to the C-terminal region of RIG-I. This cytoplasmic interaction between Riplet and RIG-I was confirmed by confocal microscopy in HeLa cells (supplemental Fig. S2). To further confirm the physical binding of Riplet to RIG-I in human cells, we carried out immunoprecipitation analyses. Full-length Riplet was co-immunoprecipitated with RIG-I (Fig. 5*B*), indicating that Riplet binds directly to RIG-I in human cells.

To determine the region responsible for the RIG-I-Riplet interaction, we constructed a RIG-I and Riplet deletion series as shown in Fig. 5*A*. Riplet-DN also bound to RIG-I (Fig. 5, *B* and *C*), indicating that the RING finger domain is dispensable for the RIG-I-Riplet interaction. This is consistent with the notion that the RING finger domain in ubiquitin ligase proteins is required for their interactions with ubiquitin-conjugating enzymes (29). Unlike TRIM25, Riplet and Riplet-DN failed to co-precipitate the two CARD domains of RIG-I (dRIG-I) (Fig. 5*D*). However, co-precipitation of the RIG-IC or RIG-RD fragments was observed (Fig. 5, *E* and *F*). RD-deleted RIG-I (RIG-I dRD) weakly associated with Riplet (Fig. 5*G*). Taken together, Riplet preferentially binds the RD and also weakly associates with the helicase region of RIG-I with its C terminus. Reporter gene analyses show that Riplet-DN only weakly suppresses RIG-I signaling and barely suppresses dRIG-I, which contains neither helicase nor RD region. Therefore, the physical interaction is correlated with the results of reporter activity.

Riplet Promotes Ubiquitination of RIG-I—Because Riplet shares 60% sequence similarity with TRIM25, we hypothesized that Riplet ubiquitinates RIG-I and that this modification leads to activation of RIG-I signaling. To test this hypothesis, we examined RIG-I ubiquitination. As expected, ubiquitination of RIG-I was increased by co-expression of Riplet under two different conditions (Fig. 6, *A* and *B*). The quantity of RIG-I ubiquitination was significantly high in the presence of Riplet (Fig. 6*C*). RIG-I ubiquitination was suppressed if Riplet was replaced with Riplet-DN (Fig. 6*D* and supplemental Fig. S4*C*). However, unlike TRIM25, Riplet binds to the C-terminal region of RIG-I. Therefore, we examined whether Riplet ubiquitinates the C-terminal region. We found that ubiquitination of RIG-IC was enhanced by Riplet expression (Fig. 6*E*). Both RIG-I dRD and RIG-I RD were also ubiquitinated by expression of Riplet (Fig. 6*F*; supplemental Fig. S4*A* and S5), suggesting that Riplet promotes ubiquitination of the helicase and RD domains of RIG-I in a manner distinct from TRIM25.

Ubiquitin is polymerized through its lysine residue. Lys-63-linked polyubiquitination is frequently observed in signal transduction pathways (30). In contrast, Lys-48-linked polyubiquitination usually leads to the degradation of protein through the proteasome. Indeed, TRIM25-mediated Lys-63-linked polyubiquitination activates the CARD-like region of RIG-I, and RNF125-mediated Lys-48-linked polyubiquitination leads to the degradation of RIG-I (23, 25). We used K48R or K63R mutated ubiquitin and found that K48R was incorporated normally into RIG-IC, whereas polyubiquitination was decreased by K63R (supplemental Fig. S4*B*). K63R mutation abolished RIG-I RD polyubiquitination by Riplet (Fig. 6*F*). These data

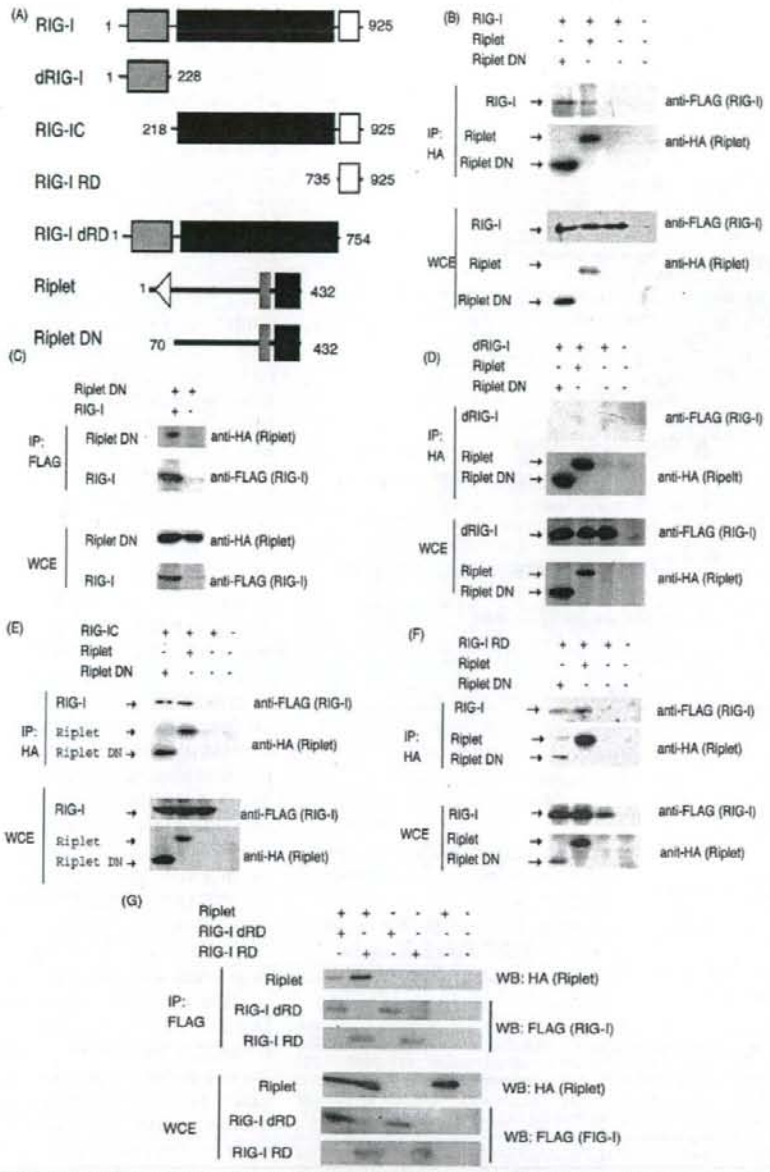

FIGURE 5. **Physical interaction of Riplet with RIG-I.** *A*, schematic representation of RIG-I or Riplet fragments used for immunoprecipitation analyses. *B*, HA-tagged Riplet (0.4 μg) or Riplet-DN (0.4 μg) were transfected into HEK293FT cells in a 6-well plate with FLAG-tagged RIG-I (0.4 μg). HA-tagged Riplet or Riplet-DN were immunoprecipitated (*IP*) with anti-HA antibodies, and samples were analyzed by Western blotting (*WB*) using an anti-FLAG or anti-HA antibody. The total amount of transfected DNA (2 μg/well) was kept constant by adding empty vector (pEF-BOS). *C*, HA-tagged Riplet-DN (0.4 μg) and FLAG-tagged RIG-I (0.4 μg) were transfected into HEK293FT cells in a 6-well plate. RIG-I was immunoprecipitated with anti-FLAG antibody, and samples were analyzed by Western blotting using an anti-FLAG or -HA antibody. The total amount of transfected DNA (2 μg/well) was kept constant by adding empty vector (pEF-BOS). *D–F*, interaction of HA-tagged Riplet or Riplet-DN with FLAG-tagged dRIG-I (*D*), RIG-IC (*E*), or RIG-I RD (*F*) was examined using immunoprecipitation assays. The proteins were expressed in HEK293FT cells, and HA-tagged Riplet was immunoprecipitated with anti-HA antibody, and samples were analyzed by Western blotting using an anti-FLAG or -HA antibody. *G*, FLAG-tagged RIG-I RD (0.4 μg) or RIG-I dRD (0.4 μg) was transfected with HA-tagged Riplet (0.4 μg) into HEK293 FT cells in a 6-well plate, and 24 h after transfection, immunoprecipitation was performed with anti-FLAG antibody and analyzed by Western blotting. The total amount of transfected DNA (2 μg/well) was kept constant by adding empty vector (pEF-BOS). *WCE*, whole cell extract.

indicates that Riplet mediates Lys-63-linked polyubiquitination of the RIG-I C-terminal helicase and RD region. Because Riplet-DN reduced the RIG-I-mediated signaling, we examined whether Riplet-DN reduced the RIG-I ubiquitination. As expected, Riplet-DN reduced RIG-I ubiquitination (Fig. 6*D* and supplemental Fig. S4*C*). These ubiquitination assay data are consistent with the notion that Riplet-mediated Lys-63-linked polyubiquitination of RIG-I is required for full activation of RIG-I signaling.

We tried to determine the ubiquitination sites of RIG-I using Lys-to-Ala (KA)-converting mutants. RIG-I has 25 Lys residues in its C-terminal region. These Lys residues of RIG-I were in turn mutated to Ala, and the degree of ubiquitination and IFN-β-inducing activity were determined with each mutant. RIG-I-mediated IFN-β promoter activation was normally augmented by co-expression of Riplet and 3KA RIG-I. Co-expression of Riplet and 5KA, however, and the ubiquitination level of RIG-I and IFN-β-inducing activity were simultaneously decreased (Fig. 7, *A* and *C*). Riplet-dependent augmentation of IFN-β promoter activation was largely suppressed when RIG-I was replaced with 5KA RIG-I (Fig. 7*B*). Therefore, Lys-849 and Lys-851 of RIG-I were crucial for RIG-I ubiquitination by Riplet. The results confirmed the importance of ubiquitination of specific Lys residues in the C-terminal region of RIG-I and for RIG-I-mediated IFN-β induction.

DISCUSSION

RIG-I plays a central role in the recognition of cytoplasmic viral RNA and is regulated by modification by small modifier ubiquitin or ubiquitin-like protein, ISG15. TRIM25 mediates Lys-63-linked polyubiquitination, which is essential for RIG-I activation (23), and RNF125 mediates Lys-48-linked polyubiquitination (25). RIG-I also harbors ISG15 modification, although the role of ISG15 modification *in vivo* remains to be deter-

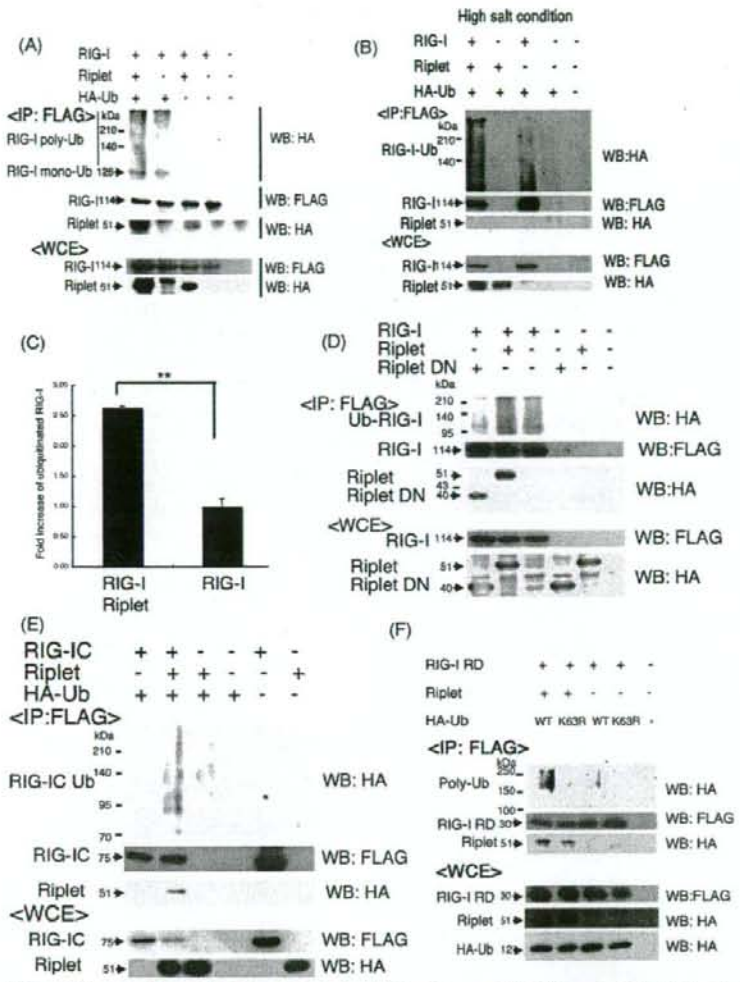

FIGURE 6. **Ubiquitination of RIG-I by Riplet.** *A* and *B*, FLAG-tagged RIG-I (0.4 μg), Riplet (0.4 μg), and HA-tagged ubiquitin (0.4 μg) expressing vectors were transfected into HEK293FT cells in 6-well plates. The total amount of transfected DNA (2 μg/well) was kept constant by adding empty vector (pEF-BOS). FLAG-tagged RIG-I was immunoprecipitated (*IP*) using an anti-FLAG antibody, and washed with the buffer containing 150 mM NaCl (*A*) or 1 M NaCl (*B*). The immunoprecipitates were separated with 8% acrylamide gel and analyzed by Western blotting (*WB*) using antibodies against HA tag (ubiquitin) or FLAG (RIG-I). Riplet was co-immunoprecipitated with FLAG-tagged RIG-I in *A* but could not co-immunoprecipitate in *B* because of high salt condition. Expression of Riplet enhanced the ubiquitination of RIG-I. Different gel conditions were employed in *A* and *B*. *C*, ubiquitinated RIG-I was quantitated with NIH image software. **, $p < 0.01$. *D*, FLAG-tagged RIG-I (0.4 μg) was transfected into HEK293 FT cells in a 6-well plate with HA-tagged Riplet (0.4 μg) or Riplet-DN (0.4 μg) and HA-tagged ubiquitin, and immunoprecipitation was carried out with anti-FLAG antibody. The total amount of transfected DNA (2 μg/well) was kept constant by adding empty vector (pEF-BOS). The samples were analyzed with 10% acrylamide gel to clearly separate Riplet from Riplet-DN and stained by Western blotting. *E*, ubiquitination of RIG-IC was also promoted by Riplet expression. HEK293FT cells were transfected with the plasmids encoding RIG-IC (0.4 μg), Riplet (0.4 μg), and/or HA-tagged ubiquitin (0.4 μg) in a 6-well plate, and 24 h after transfection, cell lysates were prepared. The total amount of transfected DNA (2 μg/well) was kept constant by adding empty vector (pEF-BOS). FLAG-tagged RIG-ICs were immunoprecipitated with anti-FLAG antibodies, and the proteins were analyzed by Western blotting. *F*, Ub-K63R are HA-tagged ubiquitin in which the lysine 3 residues were substituted with arginine. The HA-tagged Ub-K63 expressing vectors (1.2 μg), FLAG-tagged RIG-IC (0.4 μg), and/or Riplet (0.4 μg) were transfected into HEK293FT cells in 6-well plates and analyzed as shown in *A–D*. The total amount of transfected DNA (2 μg/well) was kept constant by adding empty vector (pEF-BOS). Ub-K63R was not incorporated into polyubiquitin chain of RIG-I RD. *WCE*, whole cell extract.

mined (21, 22, 31). Although Riplet and TRIM25 share 60% sequence similarity, the ubiquitination of RIG-I by Riplet is distinct from that by TRIM25; Riplet ubiquitinates the C-terminal region of RIG-I, whereas TRIM25 ubiquitinates its CARD-like region. These findings are also supported by the fact that neither Riplet nor Riplet-DN promoted or inhibited the activation of the IFN-β promoter by expression of the RIG-I CARD-like region (data not shown). It has been reported that ubiquitination of the CARD-like region of RIG-I by TRIM25 is critical for RIG-I-IPS-1 signaling (23). However, how this CARD ubiquitination is essential for activation of IPS-1 by RIG-I remains undetermined. Here we emphasize the importance of RIG-I C-terminal ubiquitination for IFN-β induction and the antiviral response. Because the C-terminal RD region inhibits the IFN inducing activity of the CARD-like region of RIG-I, it is reasonable that RIG-I C-terminal ubiquitination by Riplet inhibits the conversion from the active to inactive form of RIG-I protein after binding to viral RNA. This initial stabilization of RIG-I via ubiquitination by Riplet would provide a sufficient structure for RIG-I to maintain the accessibility to TRIM25 and facilitate TRIM25-mediated ubiquitination of the CARD-like region of RIG-I, which may lead to potential activation of IPS-1.

RIG-I is an IFN-inducible RNA helicase that is expressed at extremely low levels in resting cells (6). Initial penetration of viruses allows generation of 5′-triphosphate RNA and/or double strand RNA followed by induction of IFN-β production. This early response to viral infections triggers up-regulation of RIG-I/MDA5 and TLR3, leading to robust IFN-β production (3, 32, 33). We favor the interpretation of our present findings that during the early stages of viral infection with trace amounts of RIG-I and viral RNAs, Riplet helps host cells rearrange RIG-I conformation to activate IPS-1. This issue will need further proof because it is difficult to

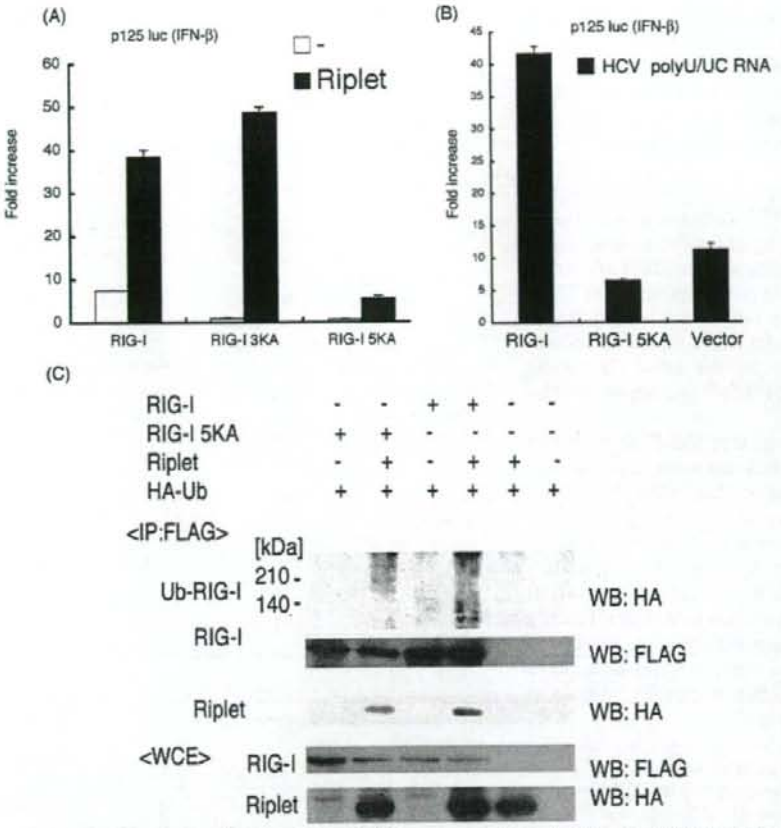

FIGURE 7. **The C-terminal two lysine residues of RIG-I are important for ubiquitination by Riplet.** *A*, RIG-I C-terminal lysine residues were substituted with alanine. RIG-I 3KA mutant protein harbors the triple mutations, K888A, K907A, and K909A. The five lysine residues, Lys-849, Lys-851, Lys-888, Lys-907, and Lys-909, were replaced with alanine in RIG-I 5KA mutant. The plasmid carrying wild-type (100 ng/well), RIG-I 3KA (100 ng/well), RIG-I 5KA (100 ng), or Riplet (100 ng) were transfected into HEK293 cells in a 24-well plate together with p125 luc reporter plasmid (100 ng/well). The amount of transfected DNA was kept constant by adding empty vector. After 24 h, the luciferase activities were measured. *B*, wild-type RIG-I (100 ng), RIG-I 5KA mutant (100 ng), or empty vector (100 ng) was transfected into HEK293 cells in a 24-well plate together with p125 luc reporter plasmids and HCV 3′-untranslated region poly(U/UC) RNA (25 ng), which is synthesized in *in vitro* transcription by T7 RNA polymerase. The amount of transfected DNA was kept constant by adding empty vector. 24 h after transfection, luciferase activities were measured. RIG-I 5KA mutant hardly responded to poly(U/UC) RNA. *C*, to observe the ubiquitinated RIG-I more clearly, we used 800 ng/well of Riplet and HA-Ub expression vector for the following transfection. HEK293FT cells in a 6-well plate were transfected with the plasmids encoding RIG-I (400 ng/well), RIG-I 5KA (400 ng/well), Riplet (800 ng/well), and/or HA-Ub (800 ng/well). The total amount of DNA was kept constant by adding the empty vector. 24 h after the transfection, the cell lysates were prepared, and the immunoprecipitation was carried out using anti-FLAG antibodies. The immunoprecipitates were analyzed by Western blotting with anti-HA or FLAG antibodies.

visualize RNRs and viral RNAs in the early infection stage and to understand the mechanisms that allow viruses to uncoat into naked viral RNA and to replicate.

We have provided several lines of evidence indicating that Riplet complements RIG-I-mediated IFN-β induction upon viral infection by both Riplet siRNA and overexpression analyses. The C-terminal lysines (849 and 851) of RIG-I are critical for Riplet-mediated RIG-I ubiquitination. However, our data indicate that Riplet alone was unable to induce IFN-β production and essentially required RIG-I to confer IFN-β induction. Furthermore, Riplet is not ubiquitously distributed over the organs tested. Ubiquitination of RIG-I induced by poly(I-C) or viruses was accelerated in cells pre-transfected with Riplet. Hence, Riplet works case-sensitive to up-regulate RIG-I antiviral activity predominantly in some organs. The physiological meaning of this response will be clarified by knock-out study.

Unexpectedly, the siRNA experiments were not robust with regard to VSV replication. Possible explanations for this are as follows: 1) the degree of gene silencing is not so profound that the proteins remain in the cells; 2) there are a number of virus-mediated IFN-inducing pathways capable of compensating each other, so that disruption of one factor does not cause a profound effect on VSV replication. Furthermore, in VSV-infected Riplet-knockdown cells, IFN-β levels were reduced even at m.o.i. = 1 (Fig. 3*D*), and accordingly, virus susceptibility was increased at m.o.i. = 0.1 (Fig. 4*C*), whereas in Riplet-overexpressing cells, antiviral activity was observed only at low m.o.i. (Fig. 4*B*). We used different transfection reagents and cell conditions in the knockdown and overexpression experiments to obtain high transfection efficiency in each. These conditional differences in knockdown and overexpression analyses might cause part of the discrepancy between the two results on Riplet antiviral activity. Another possibility to explain the apparent inconsistencies between overexpression and knockdown analyses is that high amounts of Riplet efficiently activate the RIG-I signaling, but low amounts are insufficient for RIG-I activation in high m.o.i.-infecting human cells. High amounts of Riplet with overexpressed RIG-I would confer the ability on cells to respond to very low amounts of VSV as observed in the low m.o.i. experiments. Again, *riplet* knock-out mice would reveal whether it is absolutely required for potential RIG-I activation.

How viral RNAs select RIG-I rather than dicers or the translation machinery is also unknown. During natural infection it is likely that the number of the initial invading virions would be at most several copies/cell. Uncoated viral RNA may assemble a complex consisting of viral and host molecules required for replication. We assume that cells are equipped with various

molecular arms to sensitively detect viral RNA. The molecular complexes sensing viral RNA may not be so simple that we will be able to identify more molecules than Riplet as enhancers for integral RNA recognition. In either case, yeast screening will be a good strategy to pick up such proteins in other RNA recognition systems. A molecular switch selecting IFN induction by virus RNA will then be clarified.

We show that the ubiquitination sites targeted by Riplet are the helicase and RD domains of RIG-I but not its CARD-like domains in contrast to TRIM25. Riplet may be a complement factor of the reported TRIM25 function for RIG-I activation (23). A previous report (25) failed to polyubiquitinate the RIG-I protein by TRIM25 alone. If Riplet were added to TRIM25 for RIG-I ubiquitination in the previous study, Riplet would have enabled TRIM25 to polyubiquitinate the RIG-I CARD-like region. Further studies using TRIM25 and Riplet will be required to clarify this point.

Based on our results, we propose that RIG-I-like receptors form a molecular complex that efficiently recognizes low copy numbers of viral RNA. Riplet is implicated in the RIG-I complex to enhance viral RNA response in some organs. In this context, MDA5-associated molecules might also exist in the cytoplasm to augment IFN output. Although MDA5 possesses the RD domain, it fails to recruit Riplet (data not shown) or augment IFN-β-induction in conjunction with Riplet (Fig. 2*E*). Because RLR-associated molecules naturally reside in cells and facilitate inhibition of low dose viral infection until RLRs become expressed, they may be useful therapeutic targets for an early phase antiviral immunotherapy.

Acknowledgments—We thank Dr. M. Sasai in our laboratory for technical instructions for assay of RIG-I functions and Drs. K. Shimotohno (Keio University), T. Taniguchi (University of Tokyo), and T. Fujita (Kyoto University) for their critical discussions.

REFERENCES

1. Takeuchi, O., and Akira, S. (2008) *Curr. Opin. Immunol.* **20,** 17–22
2. Honda, K., Takaoka, A., and Taniguchi, T. (2006) *Immunity* **25,** 349–360
3. Kato, H., Takeuchi, O., Sato, S., Yoneyama, M., Yamamoto, M., Matsui, K., Uematsu, S., Jung, A., Kawai, T., Ishii, K. J., Yamaguchi, O., Otsu, K., Tsujimura, T., Koh, C. S., Reis e Sousa, C., Matsuura, Y., Fujita, T., and Akira, S. (2006) *Nature* **441,** 101–105
4. Venkataraman, T., Valdes, M., Elsby, R., Kakuta, S., Caceres, G., Saijo, S., Iwakura, Y., and Barber, G. N. (2007) *J. Immunol.* **178,** 6444–6455
5. Yoneyama, M., Kikuchi, M., Matsumoto, K., Imaizumi, T., Miyagishi, M., Taira, K., Foy, E., Loo, Y. M., Gale, M., Jr., Akira, S., Yonehara, S., Kato, A., and Fujita, T. (2005) *J. Immunol.* **175,** 2851–2858
6. Yoneyama, M., Kikuchi, M., Natsukawa, T., Shinobu, N., Imaizumi, T., Miyagishi, M., Taira, K., Akira, S., and Fujita, T. (2004) *Nat. Immunol.* **5,** 730–737
7. Hornung, V., Ellegast, J., Kim, S., Brzozka, K., Jung, A., Kato, H., Poeck, H., Akira, S., Conzelmann, K. K., Schlee, M., Endres, S., and Hartmann, G. (2006) *Science* **314,** 994–997
8. Pichlmair, A., Schulz, O., Tan, C. P., Naslund, T. I., Liljestrom, P., Weber, F., and Reis e Sousa, C. (2006) *Science* **314,** 997–1001
9. Saito, T., Hirai, R., Loo, Y. M., Owen, D., Johnson, C. L., Sinha, S. C., Akira, S., Fujita, T., and Gale, M., Jr. (2007) *Proc. Natl. Acad. Sci. U. S. A.* **104,** 582–587
10. Kawai, T., Takahashi, K., Sato, S., Coban, C., Kumar, H., Kato, H., Ishii, K. J., Takeuchi, O., and Akira, S. (2005) *Nat. Immunol.* **6,** 981–988
11. Meylan, E., Curran, J., Hofmann, K., Moradpour, D., Binder, M., Bartenschlager, R., and Tschopp, J. (2005) *Nature* **437,** 1167–1172
12. Seth, R. B., Sun, L., Ea, C. K., and Chen, Z. J. (2005) *Cell* **122,** 669–682
13. Xu, L. G., Wang, Y. Y., Han, K. J., Li, L. Y., Zhai, Z., and Shu, H. B. (2005) *Mol. Cell* **19,** 727–740
14. Rothenfusser, S., Goutagny, N., DiPerna, G., Gong, M., Monks, B. G., Schoenemeyer, A., Yamamoto, M., Akira, S., and Fitzgerald, K. A. (2005) *J. Immunol.* **175,** 5260–5268
15. Loo, Y. M., Fornek, J., Crochet, N., Bajwa, G., Perwitasari, O., Martinez-Sobrido, L., Akira, S., Gill, M. A., Garcia-Sastre, A., Katze, M. G., and Gale, M., Jr. (2008) *J. Virol.* **82,** 335–345
16. Komuro, A., and Horvath, C. M. (2006) *J. Virol.* **80,** 12332–12342
17. McWhirter, S. M., Tenoever, B. R., and Maniatis, T. (2005) *Cell* **122,** 645–647
18. Saha, S. K., Pietras, E. M., He, J. Q., Kang, J. R., Liu, S. Y., Oganesyan, G., Shahangian, A., Zarnegar, B., Shiba, T. L., Wang, Y., and Cheng, G. (2006) *EMBO J.* **25,** 3257–3263
19. Kayagaki, N., Phung, Q., Chan, S., Chaudhari, R., Quan, C., O'Rourke, K. M., Eby, M., Pietras, E., Cheng, G., Bazan, J. F., Zhang, Z., Arnott, D., and Dixit, V. M. (2007) *Science* **318,** 1628–1632
20. Lin, R., Yang, L., Nakhaei, P., Sun, Q., Sharif-Askari, E., Julkunen, I., and Hiscott, J. (2006) *J. Biol. Chem.* **281,** 2095–2103
21. Zhao, C., Denison, C., Huibregtse, J. M., Gygi, S., and Krug, R. M. (2005) *Proc. Natl. Acad. Sci. U. S. A.* **102,** 10200–10205
22. Arimoto, K., Konishi, H., and Shimotohno, K. (2008) *Mol. Immunol.* **45,** 1078–1084
23. Gack, M. U., Shin, Y. C., Joo, C. H., Urano, T., Liang, C., Sun, L., Takeuchi, O., Akira, S., Chen, Z., Inoue, S., and Jung, J. U. (2007) *Nature* **446,** 916–920
24. Urano, T., Saito, T., Tsukui, T., Fujita, M., Hosoi, T., Muramatsu, M., Ouchi, Y., and Inoue, S. (2002) *Nature* **417,** 871–875
25. Arimoto, K., Takahashi, H., Hishiki, T., Konishi, H., Fujita, T., and Shimotohno, K. (2007) *Proc. Natl. Acad. Sci. U. S. A.* **104,** 7500–7505
26. Sasai, M., Shingai, M., Funami, K., Yoneyama, M., Fujita, T., Matsumoto, M., and Seya, T. (2006) *J. Immunol.* **177,** 8676–8683
27. Douglas, J., Cilliers, D., Coleman, K., Tatton-Brown, K., Barker, K., Bernhard, B., Burn, J., Huson, S., Josifova, D., Lacombe, D., Malik, M., Mansour, S., Reid, E., Cormier-Daire, V., Cole, T., and Rahman, N. (2007) *Nat. Genet.* **39,** 963–965
28. Barral, P. M., Morrison, J. M., Drahos, J., Gupta, P., Sarkar, D., Fisher, P. B., and Racaniello, V. R. (2007) *J. Virol.* **81,** 3677–3684
29. Seol, J. H., Feldman, R. M., Zachariae, W., Shevchenko, A., Correll, C. C., Lyapina, S., Chi, Y., Galova, M., Claypool, J., Sandmeyer, S., Nasmyth, K., Deshaies, R. J., Shevchenko, A., and Deshaies, R. J. (1999) *Genes Dev.* **13,** 1614–1626
30. Pickart, C. M. (2004) *Cell* **116,** 181–190
31. Kim, M. J., Hwang, S. Y., Imaizumi, T., and Yoo, J. Y. (2008) *J. Virol.* **82,** 1474–1483
32. Alexopoulou, L., Holt, A. C., Medzhitov, R., and Flavell, R. A. (2001) *Nature* **413,** 732–738
33. Tanabe, M., Kurita-Taniguchi, M., Takeuchi, K., Takeda, M., Ayata, M., Ogura, H., Matsumoto, M., and Seya, T. (2003) *Biochem. Biophys. Res. Commun.* **311,** 39–48
34. Yoneyama, M., Suhara, W., Fukuhara, Y., Fukuda, M., Nishida, E., and Fujita, T. (1998) *EMBO J.* **17,** 1087–1095

JOURNAL OF BACTERIOLOGY, Dec. 2008, p. 7918–7924 Vol. 190, No. 24
0021-9193/08/$08.00+0 doi:10.1128/JB.00911-08

The *Mycobacterium avium* Complex *gtfTB* Gene Encodes a Glucosyltransferase Required for the Biosynthesis of Serovar 8-Specific Glycopeptidolipid▽

Yuji Miyamoto,[1]* Tetsu Mukai,[1] Yumi Maeda,[1] Masanori Kai,[1] Takashi Naka,[2] Ikuya Yano,[2] and Masahiko Makino[1]

Department of Microbiology, Leprosy Research Center, National Institute of Infectious Diseases, 4-2-1 Aobacho, Higashimurayama, Tokyo 189-0002, Japan,[1] and Japan BCG Central Laboratory, 3-1-5 Matsuyama, Kiyose, Tokyo 204-0022, Japan[2]

Received 2 July 2008/Accepted 29 September 2008

***Mycobacterium avium* complex (MAC) is one of the most common opportunistic pathogens widely distributed in the natural environment. The 28 serovars of MAC are defined by variable oligosaccharide portions of glycopeptidolipids (GPLs) that are abundant on the surface of the cell envelope. These GPLs are also known to contribute to the virulence of MAC. Serovar 8 is one of the dominant serovars isolated from AIDS patients, but the biosynthesis of serovar 8-specific GPL remains unknown. To clarify this, we compared gene clusters involved in the biosynthesis of several serovar-specific GPLs and identified the genomic region predicted to be responsible for GPL biosynthesis in a serovar 8 strain. Sequencing of this region revealed the presence of four open reading frames, three unnamed genes and *gtfTB*, the function of which has not been elucidated. The simultaneous expression of *gtfTB* and two downstream genes in a recombinant *Mycobacterium smegmatis* strain genetically modified to produce serovar 1-specific GPL resulted in the appearance of 4,6-*O*-(1-carboxyethylidene)-3-*O*-methyl-glucose, which is unique to serovar 8-specific GPL, suggesting that these three genes participate in its biosynthesis. Furthermore, functional analyses of *gtfTB* indicated that it encodes a glucosyltransferase that transfers a glucose residue via 1→3 linkage to a rhamnose residue of serovar 1-specific GPL, which is critical to the formation of the oligosaccharide portion of serovar 8-specific GPL. Our findings might provide a clue to understanding the biosynthetic regulation that modulates the biological functions of GPLs in MAC.**

Mycobacteria are pathogens that cause diseases such as tuberculosis and leprosy. In addition, nontuberculous mycobacteria, which are widely distributed in the natural environment, cause opportunistic pulmonary infections resembling tuberculosis. These mycobacteria are distinguished by a multilayered cell envelope consisting of peptidoglycan, mycolyl arabinogalactan, and surface glycolipids (9, 13). The surface glycolipids are abundant and structurally different, and they may act as a barrier to immune responses (9, 13). Glycopeptidolipids (GPLs) are major glycolipid components present on the surface of several species of nontuberculous mycobacteria (40). All of these GPLs have a conserved core structure that is composed of a fatty acyl tetrapeptide glycosylated with 6-deoxytalose (6-d-Tal) and *O*-methyl-rhamnose (O-Me-Rha) and are termed non-serovar-specific GPLs (nsGPLs) (2, 4, 14). On the other hand, the GPLs of *Mycobacterium avium* complex (MAC), nontuberculous mycobacteria consisting principally of two species, *M. avium* and *M. intracellulare*, have various haptenic oligosaccharides linked to the 6-d-Tal residue of nsGPLs, resulting in serovar-specific GPLs (ssGPLs) (2, 4, 40). The oligosaccharide portions of ssGPLs define MAC serovars that are classified into 28 types. The serovar 1-specific GPL, with Rha linked to the 6-d-Tal residue, is the basic oligosaccharide unit of all ssGPLs (11). The Rha residue of serovar 1-specific GPL is further extended by various glycosylation steps, such as rhamnosylation, fucosylation, and glucosylation (11). These glycosylation steps generate structural diversity in GPLs of MAC (11). However, because of their complexity, most of the biosynthetic pathways for ssGPLs have not been fully determined. We recently showed that the biosynthesis of nsGPLs was regulated by a combination of glycosyltransferases (31). Therefore, each glycosyltransferase might mediate a specific step in the biosynthesis of ssGPLs.

In terms of biological activity, it has been reported that the properties of ssGPLs are notably different from each other and that some of the properties play a role in affecting host responses to MAC infections (3, 5, 21, 27, 37, 38). Moreover, epidemiological studies have shown that serovars 1, 4, and 8 are distributed predominantly in North America and are also frequently isolated from AIDS patients (24, 39, 41). However, in contrast to other ssGPLs, the serovar 8-specific GPL is reported to be able to induce altered immune responses (3, 21). The biosynthetic pathway for serovar 8-specific GPL, particularly its oligosaccharide portion that includes a unique 4,6-*O*-(1-carboxyethylidene)-3-*O*-methyl-glucose (Glc) residue (7, 8) that may determine the specificity of serovar 8, remains unknown (Table 1). In this study, we investigated the genomic region assumed to be associated with the biosynthesis of GPL in MAC serovar 8 strain and identified the genes involved in

* Corresponding author. Mailing address: Department of Microbiology, Leprosy Research Center, National Institute of Infectious Diseases, 4-2-1 Aobacho, Higashimurayama, Tokyo 189-0002, Japan. Phone: 81-42-391-8211. Fax: 81-42-394-9092. E-mail: yujim@nih.go.jp.
▽ Published ahead of print on 10 October 2008.

TABLE 1. Oligosaccharide structures of serovar 1- and 8-specific GPLs

Serovar	Oligosaccharide	Reference(s)
1	α-L-Rha-(1→2)-L-6-d-Tal	17
8	4,6-*O*-(1-carboxyethylidene)-3-*O*-methyl-β-D-Glc-(1→3)-α-L-Rha-(1→2)-L-6-d-Tal	7, 8

the glycosylation pathway leading to the formation of serovar 8-specific GPL.

MATERIALS AND METHODS

Bacterial strains, culture conditions, and DNA manipulation. Table 2 shows the bacterial strains and vectors used in this study. MAC strains were grown in Middlebrook 7H9 broth (Difco) with 0.05% Tween 80 supplemented with 10% Middlebrook ADC enrichment (BBL). Recombinant *M. smegmatis* strains used for GPL production were cultured in Luria-Bertani broth with 0.2% Tween 80. Isolation of DNA and transformation of *M. smegmatis* strains were performed as previously described (32). The genomic regions of MAC strains were amplified by a two-step PCR using TaKaRa *LA Taq* with GC buffer and the following program: denaturation at 98°C for 20 s and annealing-extension at 68°C for an appropriate time depending on the length of the targeted region. *Escherichia coli* strain DH5α was used for routine manipulation and propagation of plasmid DNA. When necessary, antibiotics were added as follows: kanamycin, 50 μg/ml for *E. coli* and 25 μg/ml for *M. smegmatis*; and hygromycin B, 150 μg/ml for *E. coli* and 75 μg/ml for *M. smegmatis*. Oligonucleotide primers used in this study are listed in Table 3.

Construction of expression vectors. The *rtfA* gene was amplified from genomic DNA of *M. avium* strain JATA51-01 using primers RTFA-S and RTFA-A. The PCR products were digested with each restriction enzyme and cloned into the BamHI-PstI site of pMV261 to obtain pMV-rtfA. To use the site-specific integrating mycobacterial vector more conveniently, we constructed pYM301a containing an AflII site in pYM301. The region encompassing *gtfTB*, ORF3, and ORF4 was amplified from genomic DNA of MAC serovar 8 strain ATCC 35771 using primers GTFTB-S and ORF4-A. In addition, *gtfTB* was amplified using primers GTFTB-S and GTFTB-A. The PCR products were digested with each restriction enzyme and cloned into the PstI-EcoRI site of pYM301a to obtain pYM-gtfTB-orf3-orf4 and pYM-gtfTB (Table 2).

Isolation and purification of GPLs. Harvested bacterial cells were allowed to stand in $CHCl_3$-CH_3OH (2:1, vol/vol) for several hours at room temperature. After water was added, total-lipid extracts were obtained from the organic phase and evaporated to dryness. Total-lipid extracts were subjected to mild alkaline hydrolysis as previously described (32, 33) to obtain crude GPL extracts. For analytical thin-layer chromatography (TLC), crude GPLs obtained from the same wet weight of harvested bacterial cells were spotted on Silica Gel 60 plates (Merck) using $CHCl_3$-CH_3OH-H_2O (30:8:1, vol/vol/vol) as the solvent and were visualized by spraying the plates with 10% H_2SO_4 and charring. Purified GPLs were prepared from crude GPLs by preparative TLC on the same plates, and each GPL was extracted from the corresponding band. Perdeuteriomethylation was carried out as previously described (6, 12, 17).

TABLE 3. Oligonucleotide primers used in this study

Primer	Sequence[a]	Restriction site
RTFA-S	5′-CGGGATCCCATGAAATTTGCTGTGGCAAG-3′	BamHI
RTFA-A	5′-AACTGCAGCTCAGCGACTTCGCTGCGCTTC-3′	PstI
GTFTB-S	5′-AACTGCAGAAATGACCGCCACAACCAGGGC-3′	PstI
GTFTB-A	5′-GGAATTCTCAGGCGCTCAGTGGCTCGTC-3′	EcoRI
ORF4-A	5′-GGAATTCCTAGGGCGCCAATTCGATGAG-3′	EcoRI
GTFB-U4	5′-GGAATTCGGTCGACTCGACGAAGCCGAC-3′	EcoRI
DRRC-A	5′-GGAATTCTGCAGGCGGGGCGACTCCTGCT-3′	EcoRI

[a] Underlining indicates restriction sites.

GC-MS and MALDI-TOF MS analysis. Crude and purified GPLs were hydrolyzed in 2 M trifluoroacetic acid (2 h, 120°C), and the released sugars were reduced with $NaBD_4$ and then acetylated with pyridine-acetic anhydride (1:1, vol/vol) at room temperature overnight. The resulting alditol acetates were separated and analyzed by gas chromatography-mass spectrometry (GC-MS) with a TRACE DSQ (Thermo Electron) equipped with an SP-2380 column (Supelco) using helium gas. The following program was used: temperature increased from 52 to 172°C at a rate of 40°C/min and then increased from 172 to 250°C at a rate of 3°C/min. To determine the total mass of the purified GPLs, matrix-assisted laser desorption ionization—time of flight (MALDI-TOF) mass spectra (in the positive mode) were obtained with a QSTAR XL (Applied Biosystems) using a pulse laser with emission at 337 nm. Samples mixed with 2,5-dihydroxybenzoic acid as the matrix were analyzed in the reflectron mode with an accelerating voltage of 20 kV and with operation in positive ion mode.

Nucleotide sequence accession number. The 4.6-kb genomic region amplified from MAC serovar 8 strain ATCC 35771 using primers GTFB-U4 and DRRC-A has been deposited in the DDBJ nucleotide sequence database under accession number AB437139.

RESULTS

Isolation and sequencing of the 4.6-kb genomic region responsible for GPL biosynthesis in MAC serovar 8. Lacking information on the genes responsible for biosynthesis of serovar 8-specific GPL, we compared and analyzed the genomic regions likely to be responsible for GPL biosynthesis in several

TABLE 2. Bacterial strains and vectors used in this study

Strain or vector	Characteristics	Source or reference
Bacteria		
E. coli DH5α	Cloning host	TaKaRa
M. smegmatis mc^{2}155	Expression host	35
M. intracellulare ATCC 35771	MAC serovar 8 strain	29
M. avium JATA51-01	Source of *rtfA*	17
Vectors		
pYM301	Source of pYM301a	30
pYM301a	Site-specific integrating mycobacterial vector carrying an *hsp60* promoter cassette and AflII site	This study
pMV261	*E. coli-Mycobacterium* shuttle vector carrying an *hsp60* promoter cassette	36
pMV-rtfA	pMV261 with *rtfA*	This study
pYM-gtfTB	pYM301a with *gtfTB*	This study
pYM-gtfTB-orf3-orf4	pYM301a with *gtfTB*, ORF3, and ORF4	This study

FIG. 1. Organization of the 4.6-kb genomic region isolated from MAC serovar 8 strain. Filled triangles indicate the primers used for PCR amplification.

MAC serovars (16, 28). Most of these regions have high homology to each other, while the segment between the *gtfB* and *drrC* genes was found to vary in the strains. Therefore, we assumed that this segment contains genes involved in the formation of the unique Glc residue in serovar 8-specific GPL. To clone the *gtfB-drrC* region by using PCR, we designed various primers containing sequences derived from other MAC strains. By examining combinations of several pairs of primers, a 4.6-kb fragment was amplified from genomic DNA of a MAC serovar 8 strain when primers GTFB-U4 and DRRC-A were used (Fig. 1). Sequencing of this 4.6-kb fragment revealed four complete open reading frames (Fig. 1). The deduced amino acid sequences encoded by ORF1, ORF2, ORF3, and ORF4 were found to be identical to the amino acid sequences of four functionally undefined proteins from *M. avium* strain 104, MAV_3253, MAV_3255, MAV_3256, and MAV_3257, respectively (GenBank accession no. NC_008595.1). *M. avium* strain A5 also possessed a genomic region harboring ORF2, ORF3, and ORF4 (GenBank accession no. AY130970.1). These four open reading frames are predicted to encode the following proteins: ORF1, a putative glycosyltransferase similar to GtfD, which has been identified as a fucosyltransferase involved in the biosynthesis of serovar 2-specific GPL (73% identity) (30); ORF2, a putative glycosyltransferase, designated GtfTB, showing high homology to Rv1516c of *M. tuberculosis* (61% identity) (28); ORF3, a putative polysaccharide pyruvyltransferase similar to MSMEG_4736 and MSMEG_4737 of *M. smegmatis* (61 and 58% identity, respectively) (GenBank accession no. NC_008596.1); and ORF4, a putative *O*-methyltransferase similar to MSMEG_4739 of *M. smegmatis* (55% identity) (GenBank accession no. NC_008596.1).

Identification of the genes required for synthesis of the sugar residue unique to serovar 8-specific GPL. Based on the deduced functions of the genes in the 4.6-kb fragment, we focused on *gtfTB* (ORF2), ORF3, and ORF4 and characterized them by performing expression analyses. Because the serovar 8-specific GPL has a structure in which the Rha residue of serovar 1-specific GPL is further glycosylated (Table 1), it was necessary to prepare a strain producing serovar 1-specific GPL that could be the substrate for the enzymes participating in the biosynthesis of serovar 8-specific GPL. For this, as previously demonstrated, we created a recombinant *M. smegmatis* strain, designated MS-S1, by introducing the plasmid vector pMV-rtfA having the *M. avium rtfA* gene, which converts nsGPLs to serovar 1-specific GPL (30). We then introduced the integrative expression vector pYM-gtfTB possessing *gtfTB* into MS-S1 and assessed GPL profiles by performing a TLC analysis (Fig. 2). By comparison with the profile of MS-S1/pYM301a (vector control) (Fig. 2, lane A), two new spots, designated spots GPL-SG-U and -D, were observed in MS-S1/pYM-gtfTB (Fig. 2, lane B), indicating that serovar 1-specific

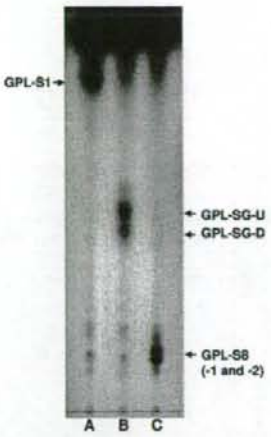

FIG. 2. TLC of crude GPL extracts from recombinant *M. smegmatis* strains MS-S1/pYM301a (A), MS-S1/pYM-gtfTB (B), and MS-S1/pYM-gtfTB-orf3-orf4 (C). GPL extracts were prepared from the total-lipid fraction, and this was followed by mild alkaline hydrolysis. Samples were spotted and developed using $CHCl_3$-CH_3OH-H_2O (30:8:1, vol/vol/vol).

GPL was converted to structurally different compounds by expression of *gtfTB*. Moreover, when the expression vector pYM-gtfTB-orf3-orf4 containing *gtfTB*, ORF3, and ORF4 was introduced into MS-S1, another new spot, designated GPL-S8, appeared (Fig. 2, lane C), implying that the structure of GPL-SG-U and -D was further modified by the products of ORF3 and ORF4. To confirm that these compounds contain the sugar residues associated with serovar 8-specific GPL, we performed a GC-MS analysis of the monosaccharides released from crude GPL extracts of each recombinant strain and the MAC serovar 8 strain (Fig. 3). The results showed that there was an excess of Glc, together with Rha, 6-d-Tal, 3,4-di-*O*-methyl-Rha, and 2,3,4-tri-*O*-methyl-Rha, in the profile of MS-S1/pYM-gtfTB compared with other profiles, as well as minor Glc peaks presumably derived from traces of trehalose-containing glycolipids (Fig. 3B). This indicates that the *gtfTB* gene mediates the transfer of a Glc residue to serovar 1-specific GPL. In contrast, the profile of MS-S1/pYM-gtfTB-orf3-orf4 revealed the presence of 4,6-*O*-(1-carboxyethylidene)-3-*O*-methyl-Glc, which was also detected in the MAC serovar 8 strain (Fig. 3C and D), demonstrating that the three genes are associated with the formation of the unique sugar residue of serovar 8-specific GPL.

Functional characterization of *gtfTB*. Expression analysis showed that serovar 1-specific GPL was converted to new compounds containing Glc when the *gtfTB* gene was expressed (Fig. 2, lane B, and Fig. 3B). Although these results suggested that the product of *gtfTB* participates in the formation of a Glc residue, it is not clear whether *gtfTB* encodes the glycosyltransferase that transfers Glc via 1→3 linkage to the Rha residue of serovar 1-specific GPL, whose linkage was previously detected in serovar 8-specific GPL (7, 8). To elucidate the function of *gtfTB*, we determined the linkage of sugar moieties of GPL-SG-U and -D, which were produced by recombinant strain

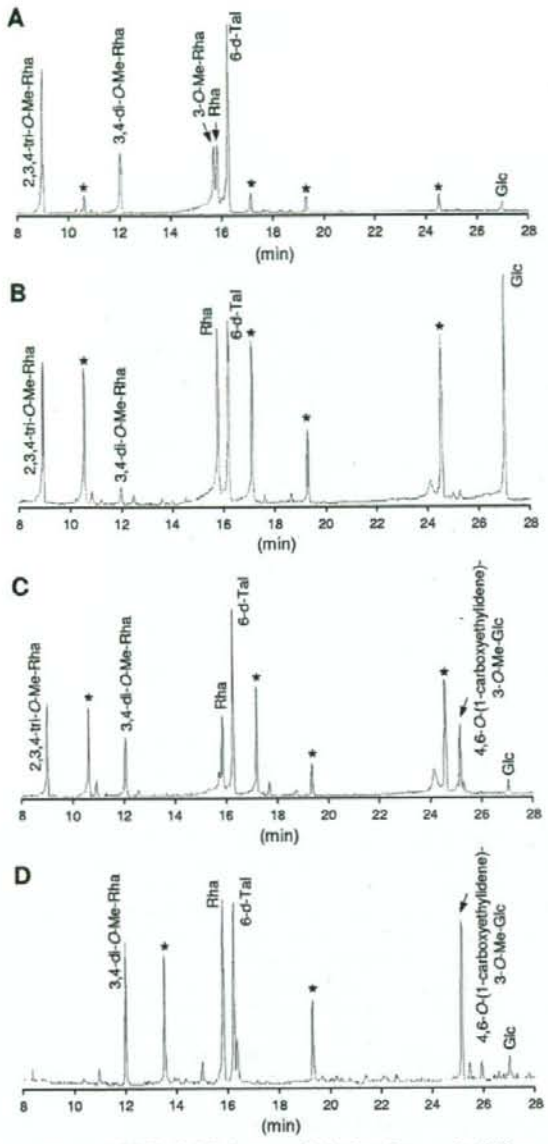

FIG. 3. GC-MS of alditol acetate derivatives from crude GPL extracts of recombinant strains *M. smegmatis* MS-S1/pYM301a (A), MS-S1/pYM-gtfTB (B), and MS-S1/pYM-gtfTB-orf3-orf4 (C) and a MAC serovar 8 strain (D). GPL extracts were prepared from the total-lipid fraction, and this was followed by mild alkaline hydrolysis. Asterisks indicate noncarbohydrates. Me, methyl.

MS-S1/pYM-gtfTB (Fig. 2, lane B). After extraction of the products from the corresponding bands on the TLC plate, purified GPL-SG-U and -D were subjected to perdeuteriomethylation followed by GC-MS. The differences in the TLC profiles of GPL-SG-U and -D might have been due to the presence or absence of fatty acid methylation, which is often observed in *M. smegmatis* GPLs (23, 31), whereas the GC-MS profiles and fragmentation ions for GPL-SG-U and -D were identical, demonstrating that GPL-SG-U and -D had the same sugar moieties and linkages. Therefore, the profiles of GPL-SG-U shown here are representative of GPL-SG-U and -D. The GC-MS profile of GPL-SG-U contained four peaks corresponding to 6-d-Tal, Rha, Glc, and 2,3,4-tri-*O*-methyl-Rha (data not shown). The characteristic spectra for Glc, Rha, and 6-d-Tal are shown in Fig. 4. The spectrum of Glc had fragment ions at *m/z* 121, 167, and 168, which represent the presence of deuteriomethyl groups at positions C-2, C-3, and C-4 (Fig. 4A). In contrast, fragment ions at *m/z* 121, 134, 193, and 240 were detected for Rha, indicating that a deuteriomethyl group was introduced at positions C-2 and C-4 of Rha, in which position C-3 was acetylated (Fig. 4B). In addition, detection of fragment ions at *m/z* 134, 181, and 193 (Fig. 4C) revealed that there was deuteriomethylation at positions C-3 and C-4 in 6-d-Tal. These results demonstrated that position C-1 of Glc is linked to position C-3 of Rha but not to position C-2 of 6-d-Tal, because it has been determined previously that position C-1 of Rha is linked to position C-2 of 6-d-Tal in the oligosaccharide of serovar 1-specific GPL (17). Accordingly, the oligosaccharide structures of GPL-SG-U and -D were determined to have Glc-(1→3)-Rha-(1→2)-6-d-Tal at D-*allo*-Thr, demonstrating that *gtfTB* encodes the glucosyltransferase that transfers a Glc residue via 1→3 linkage to the Rha residue of serovar 1-specific GPL.

Structural assignment of GPL-S8 synthesized by expression of *gtfTB*, ORF3, and ORF4. GC-MS of the crude GPL extract from MS-S1/pYM-gtfTB-orf3-orf4 revealed the presence of 4,6-*O*-(1-carboxyethylidene)-3-*O*-methyl-Glc (Fig. 3C). To confirm that this structural component was derived from GPL-S8, we performed GC-MS and MALDI-TOF MS analyses of purified GPL-S8. The results showed that GPL-S8 contained a 4,6-*O*-(1-carboxyethylidene)-3-*O*-methyl-Glc residue and two main pseudomolecular ions (*m/z* 1,565.9 and 1,579.8 $[M + Na]^+$) (data not shown). Consequently, as shown in Fig. 5, these results were consistent with the proposed structure for GPL-S8-1 and -2 containing 4,6-*O*-(1-carboxyethylidene)-3-*O*-methyl-Glc, with differences in pseudomolecular ions due to fatty acid methylation.

DISCUSSION

Structural diversity of the ssGPLs, notably in their sugar residues, defines 28 serovars of MAC. Although these ssGPLs are known to contribute to the virulence of MAC, the mechanisms of their biosynthetic regulation are largely unknown. In this study, we clarified the biosynthetic pathway for serovar 8-specific GPL, specifically the glycosylation step in which a Glc residue is transferred to the Rha residue of serovar 1-specific GPL.

To isolate the genomic region associated with the biosynthesis of serovar 8-specific GPL, we compared the GPL biosynthetic gene clusters in several MAC strains and found significant differences in the *gtfB-drrC* region. The segment flanking the 3′ end of the *gtfB-drrC* region includes several genes responsible for the serovar 1-specific GPL whose structure is found in all ssGPLs. On the other hand, it is experimentally

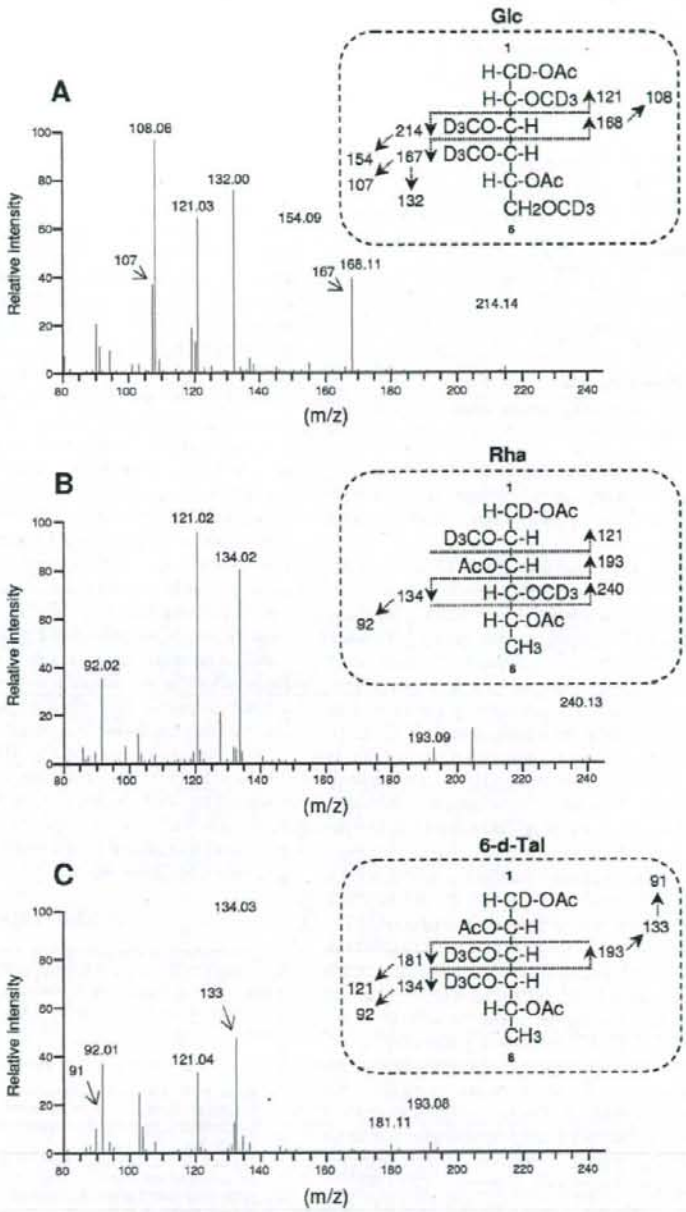

FIG. 4. GC-MS spectra and fragment ion assignments for Glc (A), Rha (B), and 6-d-Tal (C), which were derived from alditol acetates of sugars released from deuteriomethylated GPL-SG-U. Ac, acetate; D, deuterium.

clarified that the *gtfB-drrC* regions of serovar 2-, 7-, and 16-specific GPL-producing strains contain the genes involved in the formation of the specific sugar residues that are transferred to the Rha residue of serovar 1-specific GPL (18, 19, 30). Thus, this region could play an important role in generating the structural diversity of ssGPLs. As shown in this study, the specific functions for formation of sugar moieties of serovar 8-specific GPL were due to the genes present in the *gtfB-drrC*

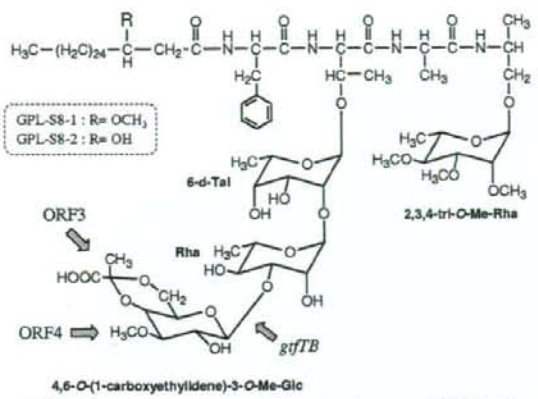

FIG. 5. Proposed structure and biosynthetic genes of GPL-S8 (serovar 8-specific GPL). Me, methyl.

region, suggesting that focusing on this region might provide clues for elucidating the characteristics of other ssGPLs whose biosynthesis is still not known.

It has been reported previously that the *gtfTB* gene in *M. avium* strains 104 and A5 was not likely to be associated with GPL biosynthesis because its ancestral homologue, Rv1516c (61% identity with the GtfTB gene), was the gene of *M. tuberculosis*, which produces no GPLs (28). Thus, it was interesting that *gtfTB* encodes a glycosyltransferase that does participate in GPL biosynthesis in which a Glc residue is transferred to serovar 1-specific GPL, yielding the serovar 8-specific GPL. *M. avium* strains 104 and A5 synthesize serovar 1-specific GPL as a final product and intermediate, respectively, while it has been recognized that neither of these strains produces serovar 8-specific GPL in spite of the presence of *gtfTB* in the GPL biosynthetic gene cluster (28). These observations raised the possibility that the transcription of *gtfTB* is inefficient in both strains due to the upstream sequences. Actually, in *M. avium* strain 104, a transposase sequence was observed upstream of *gtfTB*, indicating that this strain might be deficient in glucosylation, and consequently a serovar 1-specific GPL-producing strain is obtained (28). On the other hand, it has been shown that the biosynthetic gene cluster for serovar 7-specific GPL in *M. intracellulare* strain ATCC 35847 contains a putative glycosyltransferase gene which encodes amino acid sequences that are similar to the amino acid sequences encoded by *gtfTB* (59% identity) (18). Structural analysis of sugar moieties in serovar 7-specific GPL indicated that this GtfTB homologue may serve as a glycosyltransferase during formation of the terminal amidohexose residue that structurally resembles Glc (18).

The deduced amino acid sequences encoded by ORF3 and ORF4 showed that these genes putatively encode polysaccharide pyruvyltransferase and *O*-methyltransferase, respectively. Expression of ORF3 and ORF4 together with *gtfTB* led to structural alterations in which Glc was modified with both 4,6-*O*-(1-carboxyethylidene) and 3-*O*-methyl groups. Based on these observations, it is strongly suggested that ORF3 is associated with the formation of the 4,6-*O*-(1-carboxyethylidene) group that is synonymous with the cyclic pyruvate ketal and that ORF4 is associated with the 3-*O*-methylation of the Glc residue (Fig. 5). In mycobacteria, homologues of ORF3 and ORF4 were found only in *M. smegmatis*, as MSMEG_4736 (for ORF3), MSMEG_4737 (for ORF3), and MSMEG_4739 (for ORF4). *M. smegmatis* also produces glycolipids containing 4,6-*O*-(1-carboxyethylidene)-3-*O*-methyl-Glc as a sugar moiety (25, 34), which suggests that both homologues participate in the synthesis of these glycolipids. Sugar residues with a 4,6-*O*-(1-carboxyethylidene) group substitution have been found in carbohydrates such as extracellular polysaccharide and N-linked glycan, which are produced by some bacteria and yeasts (1, 15, 20, 22, 26). It has been shown that an increase in 4,6-*O*-(1-carboxyethylidene)-containing sugar residues leads to enhanced viscosity of extracellular polysaccharide from *Xanthomonas* sp., which alters the cell surface properties related to cellular attachment and protection from environmental stress (10). Accordingly, in terms of the properties of serovar 8-specific GPL, the presence of the 4,6-*O*-(1-carboxyethylidene) group might influence the pathogenicity of MAC serovar 8.

With regard to the antibody reactivity, it is unclear whether serovar 8-specific antibodies react with GPL-S8 because there are minor structural differences in the methylated positions of fatty acids and the terminal Rha residue linked to the tetrapeptide between GPL-S8 and serovar 8-specific GPL of MAC. Evaluation of the antibody response to GPL-S8 using serovar 8-specific antibodies would facilitate understanding the immunoreactivity mediated by ssGPLs.

In this study, we proved that *gtfTB* and adjacent genes in the GPL biosynthetic gene cluster in MAC serovar 8 strain are responsible for the formation of a unique glucose residue in serovar 8-specific GPL (Fig. 5). In particular, *gtfTB* encodes the glucosyltransferase that plays a critical role in the pathway leading from serovar 1-specific GPL to serovar 8-specific GPL. Through further study, including generation of *gtfTB* knockout mutants of MAC serovar 8 strains, results relevant to the biosynthesis of serovar 8-specific GPL might help clarify the biological function of ssGPLs and their role in the host-pathogen relationships of MAC.

ACKNOWLEDGMENTS

This study was supported in part by a Grant-in-Aid for Young Scientists (B) from the Ministry of Education, Culture, Science and Technology of Japan and Research on Emerging and Re-Emerging Infectious Diseases from the Ministry of Health, Labor and Welfare of Japan.

REFERENCES

1. **Aman, P., M. McNeil, L.-E. Franzen, A. G. Darvill, and P. Albersheim.** 1981. Structural elucidation, using HPLC-MS and GLC-MS, of the acidic exopolysaccharide secreted by *Rhizobium meliloti* strain Rm1021. Carbohydr. Res. **95**:263–282.
2. **Aspinall, G. O., D. Chatterjee, and P. J. Brennan.** 1995. The variable surface glycolipids of mycobacteria: structures, synthesis of epitopes, and biological properties. Adv. Carbohydr. Chem. Biochem. **51**:169–242.
3. **Barrow, W. W., T. L. Davis, E. L. Wright, V. Labrousse, M. Bachelet, and N. Rastogi.** 1995. Immunomodulatory spectrum of lipids associated with *Mycobacterium avium* serovar 8. Infect. Immun. **63**:126–133.
4. **Belisle, J. T., K. Klaczkiewicz, P. J. Brennan, W. R. Jacobs, Jr., and J. M. Inamine.** 1993. Rough morphological variants of *Mycobacterium avium*. Characterization of genomic deletions resulting in the loss of glycopeptidolipid expression. J. Biol. Chem. **268**:10517–10523.
5. **Bhatnagar, S., and J. S. Schorey.** 2007. Exosomes released from infected macrophages contain *Mycobacterium avium* glycopeptidolipids and are proinflammatory. J. Biol. Chem. **282**:25779–25789.
6. **Bjorndal, H., C. G. Hellerqvist, B. Lindberg, and S. Svensson.** 1970. Gas-liquid chromatography and mass spectrometry in methylation analysis of polysaccharides. Angew. Chem. Int. Ed. Engl. **9**:610–619.

7. **Brennan, P. J., G. O. Aspinall, and J. E. Shin.** 1981. Structure of the specific oligosaccharides from the glycopeptidolipid antigens of serovars in the *Mycobacterium avium-Mycobacterium intracellulare-Mycobacterium scrofulaceum* complex. J. Biol. Chem. **256**:6817–6822.
8. **Brennan, P. J., H. Mayer, G. O. Aspinall, and J. E. Nam Shin.** 1981. Structures of the glycopeptidolipid antigens from serovars in the *Mycobacterium avium/Mycobacterium intracellulare/Mycobacterium scrofulaceum* serocomplex. Eur. J. Biochem. **115**:7–15.
9. **Brennan, P. J., and H. Nikaido.** 1995. The envelope of mycobacteria. Annu. Rev. Biochem. **64**:29–63.
10. **Casas, J. A., V. E. Santos, and F. Garcia-Ochoa.** 2000. Xanthan gum production under several operational conditions: molecular structure and rheological properties. Enzyme Microb. Technol. **26**:282–291.
11. **Chatterjee, D., and K. H. Khoo.** 2001. The surface glycopeptidolipids of mycobacteria: structures and biological properties. Cell. Mol. Life Sci. **58**: 2018–2042.
12. **Ciucanu, I., and F. Kerek.** 1984. A simple and rapid method for the permethylation of carbohydrates. Carbohydr. Res. **131**:209–217.
13. **Daffe, M., and P. Draper.** 1998. The envelope layers of mycobacteria with reference to their pathogenicity. Adv. Microb. Physiol. **39**:131–203.
14. **Daffe, M., M. A. Laneelle, and G. Puzo.** 1983. Structural elucidation by field desorption and electron-impact mass spectrometry of the C-mycosides isolated from *Mycobacterium smegmatis*. Biochim. Biophys. Acta **751**:439–443.
15. **D'Haeze, W., J. Glushka, R. De Rycke, M. Holsters, and R. W. Carlson.** 2004. Structural characterization of extracellular polysaccharides of *Azorhizobium caulinodans* and importance for nodule initiation on *Sesbania rostrata*. Mol. Microbiol. **52**:485–500.
16. **Eckstein, T. M., J. T. Belisle, and J. M. Inamine.** 2003. Proposed pathway for the biosynthesis of serovar-specific glycopeptidolipids in *Mycobacterium avium* serovar 2. Microbiology **149**:2797–2807.
17. **Eckstein, T. M., F. S. Silbaq, D. Chatterjee, N. J. Kelly, P. J. Brennan, and J. T. Belisle.** 1998. Identification and recombinant expression of a *Mycobacterium avium* rhamnosyltransferase gene (*rfbA*) involved in glycopeptidolipid biosynthesis. J. Bacteriol. **180**:5567–5573.
18. **Fujiwara, N., N. Nakata, S. Maeda, T. Naka, M. Doe, I. Yano, and K. Kobayashi.** 2007. Structural characterization of a specific glycopeptidolipid containing a novel *N*-*acyl*-deoxy sugar from *Mycobacterium intracellulare* serotype 7 and genetic analysis of its glycosylation pathway. J. Bacteriol. **189**:1099–1108.
19. **Fujiwara, N., N. Nakata, T. Naka, I. Yano, M. Doe, D. Chatterjee, M. McNeil, P. J. Brennan, K. Kobayashi, M. Makino, S. Matsumoto, H. Ogura, and S. Maeda.** 2008. Structural analysis and biosynthesis gene cluster of an antigenic glycopeptidolipid from *Mycobacterium intracellulare*. J. Bacteriol. **190**:3613–3621.
20. **Gemmill, T. R., and R. B. Trimble.** 1996. *Schizosaccharomyces pombe* produces novel pyruvate-containing N-linked oligosaccharides. J. Biol. Chem. **271**:25945–25949.
21. **Horgen, L., E. L. Barrow, W. W. Barrow, and N. Rastogi.** 2000. Exposure of human peripheral blood mononuclear cells to total lipids and serovar-specific glycopeptidolipids from *Mycobacterium avium* serovars 4 and 8 results in inhibition of TH1-type responses. Microb. Pathog. **29**:9–16.
22. **Jansson, P. E., L. Kenne, and B. Lindberg.** 1975. Structure of extracellular polysaccharide from *Xanthomonas campestris*. Carbohydr. Res. **45**:275–282.
23. **Jeevarajah, D., J. H. Patterson, M. J. McConville, and H. Billman-Jacobe.** 2002. Modification of glycopeptidolipids by an *O*-methyltransferase of *Mycobacterium smegmatis*. Microbiology **148**:3079–3087.
24. **Julander, I., S. Hoffner, B. Petrini, and L. Ostlund.** 1996. Multiple serovars of *Mycobacterium avium* complex in patients with AIDS. APMIS **104**:318–320.
25. **Kamisango, K., S. Saadat, A. Dell, and C. E. Ballou.** 1985. Pyruvylated glycolipids from *Mycobacterium smegmatis*. Nature and location of the lipid components. J. Biol. Chem. **260**:4117–4121.
26. **Kojima, N., S. Kaya, Y. Araki, and E. Ito.** 1988. Pyruvic-acid-containing polysaccharide in the cell wall of *Bacillus polymyxa* AHU 1385. Eur. J. Biochem. **174**:255–260.
27. **Krzywinska, E., S. Bhatnagar, L. Sweet, D. Chatterjee, and J. S. Schorey.** 2005. *Mycobacterium avium* 104 deleted of the methyltransferase D gene by allelic replacement lacks serotype-specific glycopeptidolipids and shows attenuated virulence in mice. Mol. Microbiol. **56**:1262–1273.
28. **Krzywinska, E., and J. S. Schorey.** 2003. Characterization of genetic differences between *Mycobacterium avium* subsp. *avium* strains of diverse virulence with a focus on the glycopeptidolipid biosynthesis cluster. Vet. Microbiol. **91**:249–264.
29. **Li, Z., G. H. Bai, C. F. von Reyn, P. Marino, M. J. Brennan, N. Gine, and S. L. Morris.** 1996. Rapid detection of *Mycobacterium avium* in stool samples from AIDS patients by immunomagnetic PCR. J. Clin. Microbiol. **34**:1903–1907.
30. **Miyamoto, Y., T. Mukai, Y. Maeda, N. Nakata, M. Kai, T. Naka, I. Yano, and M. Makino.** 2007. Characterization of the fucosylation pathway in the biosynthesis of glycopeptidolipids from *Mycobacterium avium* complex. J. Bacteriol. **189**:5515–5522.
31. **Miyamoto, Y., T. Mukai, N. Nakata, Y. Maeda, M. Kai, T. Naka, I. Yano, and M. Makino.** 2006. Identification and characterization of the genes involved in glycosylation pathways of mycobacterial glycopeptidolipid biosynthesis. J. Bacteriol. **188**:86–95.
32. **Miyamoto, Y., T. Mukai, F. Takeshita, N. Nakata, Y. Maeda, M. Kai, and M. Makino.** 2004. Aggregation of mycobacteria caused by disruption of fibronectin-attachment protein-encoding gene. FEMS Microbiol. Lett. **236**:227–234.
33. **Patterson, J. H., M. J. McConville, R. E. Haites, R. L. Coppel, and H. Billman-Jacobe.** 2000. Identification of a methyltransferase from *Mycobacterium smegmatis* involved in glycopeptidolipid synthesis. J. Biol. Chem. **275**:24900–24906.
34. **Saadat, S., and C. E. Ballou.** 1983. Pyruvylated glycolipids from *Mycobacterium smegmatis*. Structures of two oligosaccharide components. J. Biol. Chem. **258**:1813–1818.
35. **Snapper, S. B., R. E. Melton, S. Mustafa, T. Kieser, and W. R. Jacobs, Jr.** 1990. Isolation and characterization of efficient plasmid transformation mutants of *Mycobacterium smegmatis*. Mol. Microbiol. **4**:1911–1919.
36. **Stover, C. K., V. F. de la Cruz, T. R. Fuerst, J. E. Burlein, L. A. Benson, L. T. Bennett, G. P. Bansal, J. F. Young, M. H. Lee, G. F. Hatfull, S. B. Snapper, R. G. Barletta, W. R. Jacobs, Jr., and B. R. Bloom.** 1991. New use of BCG for recombinant vaccines. Nature **351**:456–460.
37. **Sweet, L., and J. S. Schorey.** 2006. Glycopeptidolipids from *Mycobacterium avium* promote macrophage activation in a TLR2- and MyD88-dependent manner. J. Leukoc. Biol. **80**:415–423.
38. **Tassell, S. K., M. Pourshafie, E. L. Wright, M. G. Richmond, and W. W. Barrow.** 1992. Modified lymphocyte response to mitogens induced by the lipopeptide fragment derived from *Mycobacterium avium* serovar-specific glycopeptidolipids. Infect. Immun. **60**:706–711.
39. **Tsang, A. Y., J. C. Denner, P. J. Brennan, and J. K. McClatchy.** 1992. Clinical and epidemiological importance of typing of *Mycobacterium avium* complex isolates. J. Clin. Microbiol. **30**:479–484.
40. **Vergne, I., and M. Daffe.** 1998. Interaction of mycobacterial glycolipids with host cells. Front. Biosci. **3**:d865–876.
41. **Yakrus, M. A., and R. C. Good.** 1990. Geographic distribution, frequency, and specimen source of *Mycobacterium avium* complex serotypes isolated from patients with acquired immunodeficiency syndrome. J. Clin. Microbiol. **28**:926–929.

The Clathrin-Mediated Endocytic Pathway Participates in dsRNA-Induced IFN-β Production[1]

Kiyoharu Itoh,[2] Ayako Watanabe,[2] Kenji Funami,[3] Tsukasa Seya, and Misako Matsumoto[4]

TLR3 and cytoplasmic RIG-I-like receptor (RLR) recognize virus-derived dsRNA and induce type I IFN production in a distinct manner. Human TLR3 localizes to the endosomal compartments in myeloid dendritic cells (mDCs), while it localizes to both the cell surface and interior in fibroblasts and epithelial cells. TLR3 signaling arises in the intracellular compartment in both cell types and requires endosomal maturation. The mechanisms by which extracellular dsRNA is delivered to the TLR3-containing organelle remain largely unknown. Among various synthetic dsRNAs, poly(I:C) is preferentially internalized and activates TLR3 in mDCs. In vitro transcribed dsRNAs hardly induce IFN-β production in mDCs. In this study, we demonstrate that the clathrin-dependent endocytic pathway mediates cell entry of poly(I:C) to induce IFN-β gene transcription. Furthermore, poly(I:C)-induced IFN-β production is inhibited by pretreatment of cells with B- and C-type oligodeoxynucleotides (ODNs) but not with TLR7/8 ligands. The binding and internalization of B-type ODNs by mDCs was reduced in the presence of poly(I:C), suggesting that poly(I:C) shares the uptake receptor with B- and C-type ODNs. Hence, foreign dsRNA is recognized by differently categorized receptors, cytoplasmic RIG-I-like receptor, membrane-bound TLR3 and cell-surface RNA capture. The endocytic pathway is critical for dsRNA-induced TLR3-mediated cell activation. *The Journal of Immunology,* **2008, 181: 5522–5529.**

Type I IFNs (IFN-α/β) play essential roles in both innate and adaptive antiviral immune responses (1, 2). Many types of cells such as fibroblasts, epithelial cells, and dendritic cells (DCs)[5] produce IFN-β upon viral infection or stimulation with poly(I:C), a synthetic analog of viral dsRNA (3). Membrane-bound TLR3 and cytoplasmic DEAD/H box RNA helicases, such as retinoic acid-inducible gene-I and melanoma differentiation-associated gene 5, participate in the recognition of virus-derived dsRNA and induction of IFN-α/β gene transcription (4–9).

Human TLR3 localizes to the endosomal compartments in myeloid DCs (mDCs), while it localizes to both the cell-surface and interior of fibroblasts and epithelial cells (5, 10, 11). Anti-human TLR3 mAb inhibits poly(I:C)-induced IFN-β production in fibroblasts, indicating that TLR3 present on the cell surface participates in dsRNA recognition (5). However, in both cell types, TLR3 signaling arises in an intracellular compartment and requires endosomal maturation (10, 11). After dsRNA recognition, TLR3 homodimerizes, and this is followed by recruitment of an adaptor molecule, i.e., Toll-IL-1 receptor domain-containing adaptor molecule-1 (TICAM-1, also called Toll-IL-1 receptor domain-containing adaptor inducing IFN-β). This activates the NF-κB and interferon regulatory factor-3 transcription factors leading to IFN-β production (12–15). However, the mechanism by which extracellular dsRNA is delivered to the TLR3-positive organelle is unknown.

A recent study has shown that CD14 directly binds to poly(I:C) and mediates poly(I:C) cellular uptake (16). Bone marrow-derived macrophages from CD14$^{-/-}$ mice exhibited impaired responses to poly(I:C) (16). CD14 is a well-known cell-surface pattern-recognition receptor that is involved in both LPS-mediated TLR4 signaling and in TLR2 signaling (17, 18). However, mDCs do not express CD14 (19), suggesting that other cell-surface molecules mediate the entry of dsRNA into mDCs. In this study, we used pharmacological inhibitors to analyze the mechanisms by which extracellular dsRNAs activate endosomal TLR3. We found that the clathrin-dependent endocytic pathway participates in poly(I:C)-induced IFN-β production in mDCs. Furthermore, an inhibition study with various nucleic acids revealed that poly(I:C) shares its uptake receptor with B- and C-type oligodeoxynucleotides (ODNs).

Materials and Methods

Cell culture and reagents

A human embryonic kidney cell line HEK293 was obtained from Sumitomo Pharmaceuticals and maintained in DMEM supplemented with 10% heat-inactivated FCS (JRH Biosciences) and antibiotics. The HEK293 cells have no TLR3. We prepared TLR3-expressing HEK293 cells by transient transfection of the expression plasmid for human TLR3, which predominantly express TLR3 intracellularly but possess some TLR3 molecules on the cell-surface. Chloroquine, chlorpromazine, cytochalasin D, methyl-β-cyclodextrin, 4′,6-diamidino-2-phenylindole (DAPI), propidium iodide, control ODN2006, LPS from *Escherichia coli* (serotype 0111:B4), and polymyxin B were purchased from Sigma-Aldrich. Alexa Fluor 488-acetylated low-density lipoprotein (AcLDL) and Alexa Fluor 488-cholera toxin B subunit (CTXB) were from Molecular Probes. Poly(I:C) was

Department of Microbiology and Immunology, Hokkaido University Graduate School of Medicine, Kita 15, Nishi 7, Kita-ku, Sapporo, Japan

Received for publication May 27, 2008. Accepted for publication August 12, 2008.

The costs of publication of this article were defrayed in part by the payment of page charges. This article must therefore be hereby marked *advertisement* in accordance with 18 U.S.C. Section 1734 solely to indicate this fact.

[1] This work was supported in part by Grants-in-Aid from the Ministry of Education, Science, and Culture, the Ministry of Health, Labor, and Welfare of Japan, and by the Uehara Memorial Foundation, the Mitsubishi Foundation, the NorthTec Foundation, and the Akiyama Foundation. Financial supports by the Sapporo Biocluster "Bio-S" the Knowledge Cluster Initiative of the MEXT, and the Program of Founding Research Centers for Emerging and Reemerging Infectious Diseases, MEXT are gratefully acknowledged.

[2] K. Itoh and A. Watanabe contributed equally to this work.

[3] Current address: Center for Integrated Medical Research, Keio University, Tokyo, Japan.

[4] Address correspondence and reprint requests to Dr. Misako Matsumoto, Department of Microbiology and Immunology, Hokkaido University Graduate School of Medicine, Kita 15, Nishi 7, Kita-ku, Sapporo, Japan. E-mail address: matumoto@pop.med.hokudai.ac.jp

[5] Abbreviations used in this paper: DC, dendritic cell; mDC, myeloid DC; TICAM-1, Toll-IL-1 receptor-containing adaptor molecule-1; ODN, oligodeoxynucleotide; AcLDL, acetylated low density lipoprotein; CTXB, cholera toxin subunit B; MV, measles virus; CIAP, calf intestine alkaline phosphatase; iDC, immature DC; pDC, plasmacytoid DC; CpG-B, B-type CpG ODN; CpG-A, a-type CpG ODN; DPBS, Dulbecco's PBS; DOTAP, *N*-[1-(2,3-dioleoyloxy)propyl]-*N*,*N*,*N*-trimethylammonium methyl sulfate; DAPI, 4′,6-diamidino-2-phenylindole.

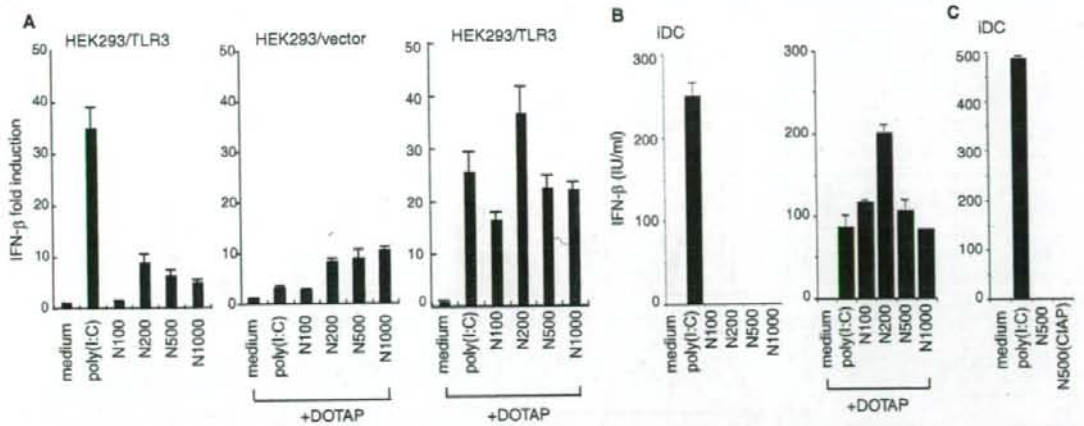

FIGURE 1. Unresponsiveness of mDCs to extracellular in vitro transcribed dsRNA. *A*, IFN-β promoter activation in HEK293 cells expressing TLR3 in response to poly(I:C) and MV-derived synthetic dsRNAs. *Left panel*, HEK293 cells in 24-well plates were transfected with pEFBOS/hTLR3 together with the reporter plasmid. Twenty-four hours after transfection, cells were stimulated with 10 μg/ml poly(I:C) or in vitro transcribed MV-originated dsRNA (N100, N200, N500, or N1000); *center and right panels*, HEK293 cells transfected with pEFBOS (*center panel*) or pEFBOS/hTLR3 (*right panel*) were stimulated with 5 μg/ml dsRNAs complexed with DOTAP. After 6 h, the luciferase reporter activities were measured and expressed as the fold induction relative to the activity of unstimulated cells. Representative data from a minimum of three separate experiments are shown. HEK293 cells transfected with pEFBOS did not respond to extracellular MV-originated dsRNAs (data not shown). *B*, IFN-β production in monocyte-derived iDCs stimulated with dsRNA. *Left panel*, Monocyte-derived iDCs (1×10^6/ml) were stimulated with 10 μg/ml poly(I:C) or in vitro transcribed MV-originated dsRNA; *right panel*, Monocyte-derived iDCs (6×10^5/ml) were stimulated with 5 μg/ml dsRNAs complexed with DOTAP and cultured for 24 h. *C*, Monocyte-derived iDCs (1×10^6/ml) were exogenously stimulated with 10 μg/ml N500 or CIAP-treated N500. After 24 h, the amount of IFN-β present in the culture supernatant was assessed by an ELISA kit. Representative data from a minimum of three separate experiments are shown.

from Amersham Bioscience. Imiquimod, Gardiquimod, CL075, ODN2006, ODN2216, ODNM362, FITC-ODN2006, and FITC-ODN2216 were purchased from Invivogen. Poly I was provided from Dr. Nishikawa (Institute for Biological Resources and Function, Tsukuba, Japan). Anti-human TLR3 mAb (clone TLR3.7) was generated in our laboratory (5). Anti-dsRNA mAb (K1) (20) was purchased from BioLink. Mouse IgG1 and mouse IgG2a were from Sigma-Aldrich, anti-CD83 mAb was from Ancell, Alexa Fluor568-conjugated goat anti-mouse IgG was from Molecular Probes, and FITC-labeled goat anti-mouse IgG was from American Qualex. Cytochalasin D was dissolved in DMSO at the concentration of 1 mg/ml.

dsRNA

dsRNAs of various lengths (N100, N200, N500, and N1000) were synthesized using a MEGAscript RNA Kit (Ambion) as described previously (21). cDNA of the N-protein of the measles virus (MV) strain Edmonston was used as a template for the transcription reaction. The synthetic dsRNAs were treated with polymyxin B (final 10 μg/ml) for 1 h at 37°C before stimulation of the cells. Treatment of dsRNA with calf intestine alkaline phosphatase (CIAP) was performed as described (22). In brief, 10 μg dsRNA was treated with 30 U CIAP (Roche) for 3 h at 37°C in the presence of 10 U RNase inhibitor (Promega). The enzyme was removed by using the RNeasy Mini kit (Qiagen).

Cytokine assay

$CD14^+$ monocytes were isolated from human PBMCs using the MACS system (Miltenyi Biotec). The monocytes were cultured for 6 days in RPMI 1640 supplemented with 10% heat-inactivated FCS and antibiotics in the presence of 500 U/ml GM-CSF and 100 U/ml IL-4 (PeproTech) to obtain monocyte-derived immature DCs (iDCs) (19). iDCs in 96-well round-bottom plates (1×10^6/ml) were stimulated with synthetic duplex RNA or poly(I:C) for 24 h in the presence of 500 U/ml GM-CSF. The amount of IFN-β present in the culture supernatants was measured by ELISA kit (TFB). In some experiments, dsRNA (1 μg) was mixed with 6 μl of *N*-[1-(2,3-dioleoyloxy)propyl]-*N*,*N*,*N*-trimethylammonium methyl sulfate (DOTAP) (Roche) in OPTI-MEM (total 30 μl) and incubated for 10 min at room temperature. The mixture was added to iDCs (6×10^5/ml). In the case of inhibition assays, cells were preincubated with indicated concentrations of pharmacological inhibitors or nucleic acids for 1 h at 37°C and then stimulated with 10 μg/ml poly(I:C) for 24 h. At the time of supernatant collection, cells were washed twice with Dulbecco's PBS (DPBS) and then stained with propidium iodide (50 μg/ml in DPBS) for 10 min at room temperature. The viability of the cells was estimated by flow cytometry.

Assay for clathrin-dependent and independent endocytosis

iDCs and HEK293 cells were pretreated with chlorpromazine (25 μg/ml for iDCs, 50 μg/ml for HEK293 cells), methyl-β-cyclodextrin (1 mM), or medium alone for 1 h at 37°C and subsequently incubated with Alexa Fluor 488-AcLDL (0.2 μM for iDC, 0.02 μM for HEK293) or Alexa Fluor 488-CTXB (5 μg/ml for iDC, 50 μg/ml for HEK293) for 30 min at 4°C. The cells were then warmed for 5 min at 37°C to allow endocytosis to occur (23). For quenching the fluorescence of uningested Alexa Fluor 488-AcLDL or Alexa Fluor 488-CTXB, the cell suspensions were mixed with trypan blue solution (2 mg/ml in DPBS) and analyzed by flow cytometry (19).

Complementary DNA expression vector

Complementary DNA for human TLR3 was cloned in our laboratory by RT-PCR and was ligated into the cloning site of the expression vector pEFBOS, a gift from Dr. S. Nagata (Osaka University, Osaka, Japan).

Reporter gene assay

HEK293 cells (2×10^5 cells per well) seeded in 24-well plates were transiently transfected with pEFBOS/TLR3 (0.1 μg) or empty vector together with a luciferase-linked p-125 luc reporter plasmid (0.1 μg) using Lipofectamine 2000 reagent (Invitrogen). The p-125 luc reporter containing the human IFN-β promoter region (−125 to +19) was provided by Dr. T. Taniguchi (University of Tokyo, Tokyo, Japan). The total amount of transfected DNA (0.8 μg) was kept constant by adding empty vector. The plasmid phRL-TK (2.5 ng) was used as an internal control. Twenty-four hours after transfection, cells were washed and stimulated with medium alone or polymyxin B-treated dsRNA for 6 h. In some experiments, cells were incubated with dsRNA complexed with DOTAP for 6 h. In the inhibition assays, cells were preincubated with inhibitors or nucleic acids for 1 h at 37°C and then stimulated with 10 μg/ml poly(I:C) for 6 h. The cells were lysed in lysis buffer (Promega), and dual luciferase activities were measured according to the manufacturer's instructions. The firefly luciferase activity was normalized by *Renella* luciferase activitiy and is expressed as the fold induction relative to the activity of unstimulated vector-transfected cells.